

Quantum Criticality and Black Holes



Talk online: sachdev.physics.harvard.edu



Particle theorists

Sean Hartnoll, KITP

Christopher Herzog, Princeton

Pavel Kovtun, Victoria

Dam Son, Washington

Condensed matter
theorists



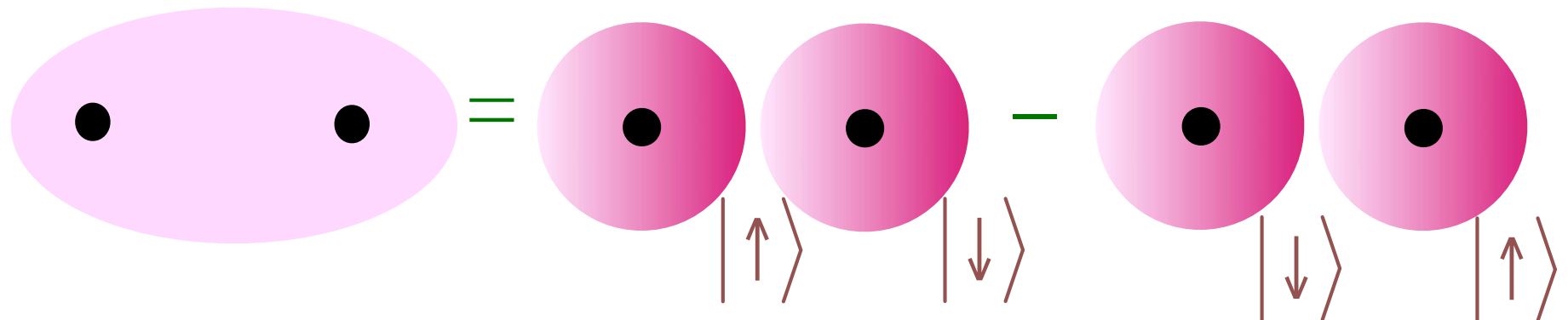
Markus Mueller, Harvard

Subir Sachdev, Harvard

Quantum Entanglement



Hydrogen molecule:



$$= \frac{1}{\sqrt{2}} (|\uparrow\downarrow\rangle - |\downarrow\uparrow\rangle)$$

Superposition of two electron states leads to non-local correlations between spins

Quantum Phase Transition

Change in the nature of entanglement in a macroscopic quantum system.

Familiar phase transitions, such as water boiling to steam, also involve macroscopic changes, but in thermal motion

Quantum Criticality

The complex and non-local entanglement at the critical point between two quantum phases

Outline

1. Entanglement of spins

Experiments on antiferromagnetic insulators

2. Black Hole Thermodynamics

Connections to quantum criticality

3. Nernst effect in the cuprate superconductors

Quantum criticality and dyonic black holes

4. Quantum criticality in graphene

Hydrodynamic cyclotron resonance and Nernst effect

Outline

1. Entanglement of spins

Experiments on antiferromagnetic insulators

2. Black Hole Thermodynamics

Connections to quantum criticality

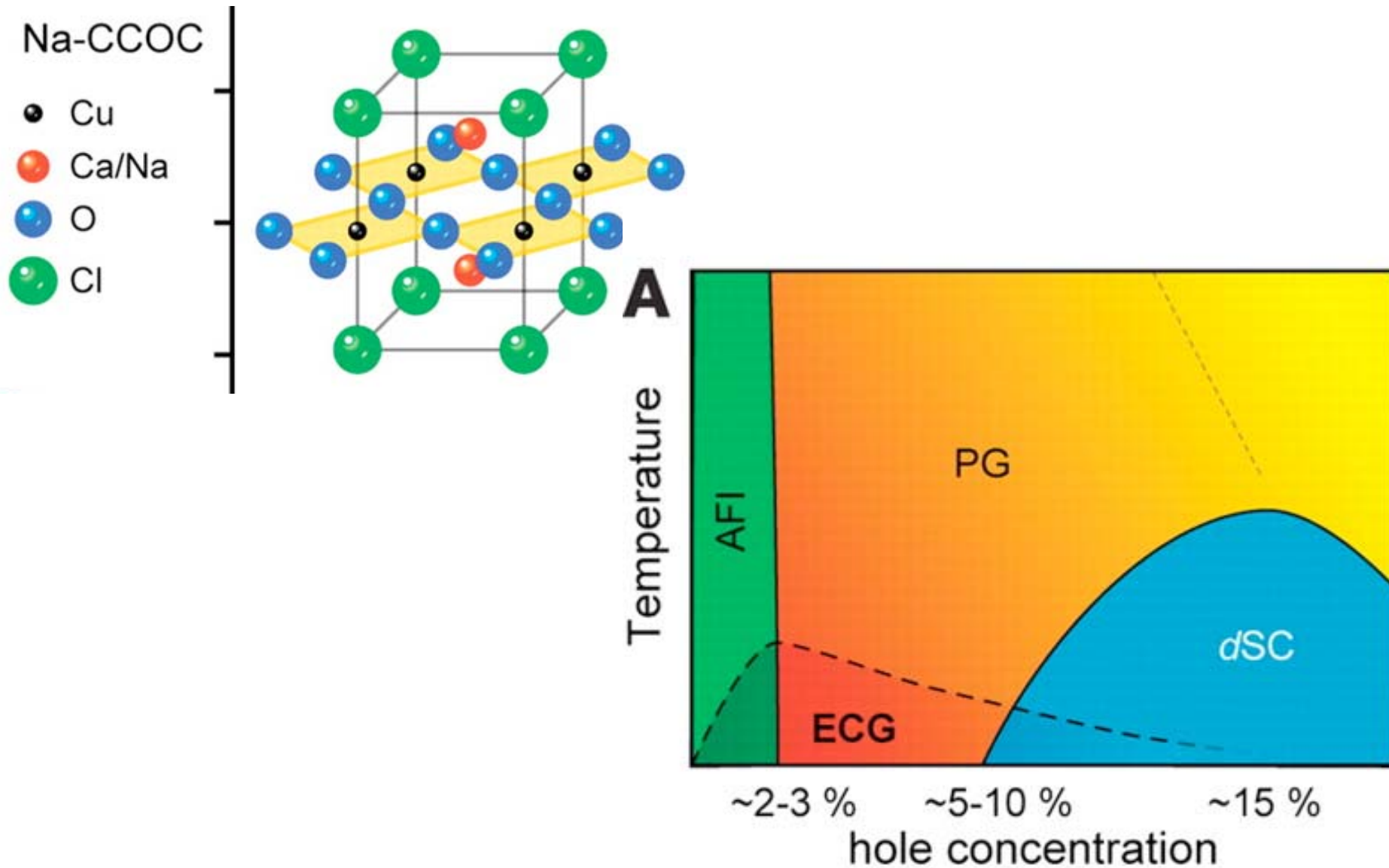
3. Nernst effect in the cuprate superconductors

Quantum criticality and dyonic black holes

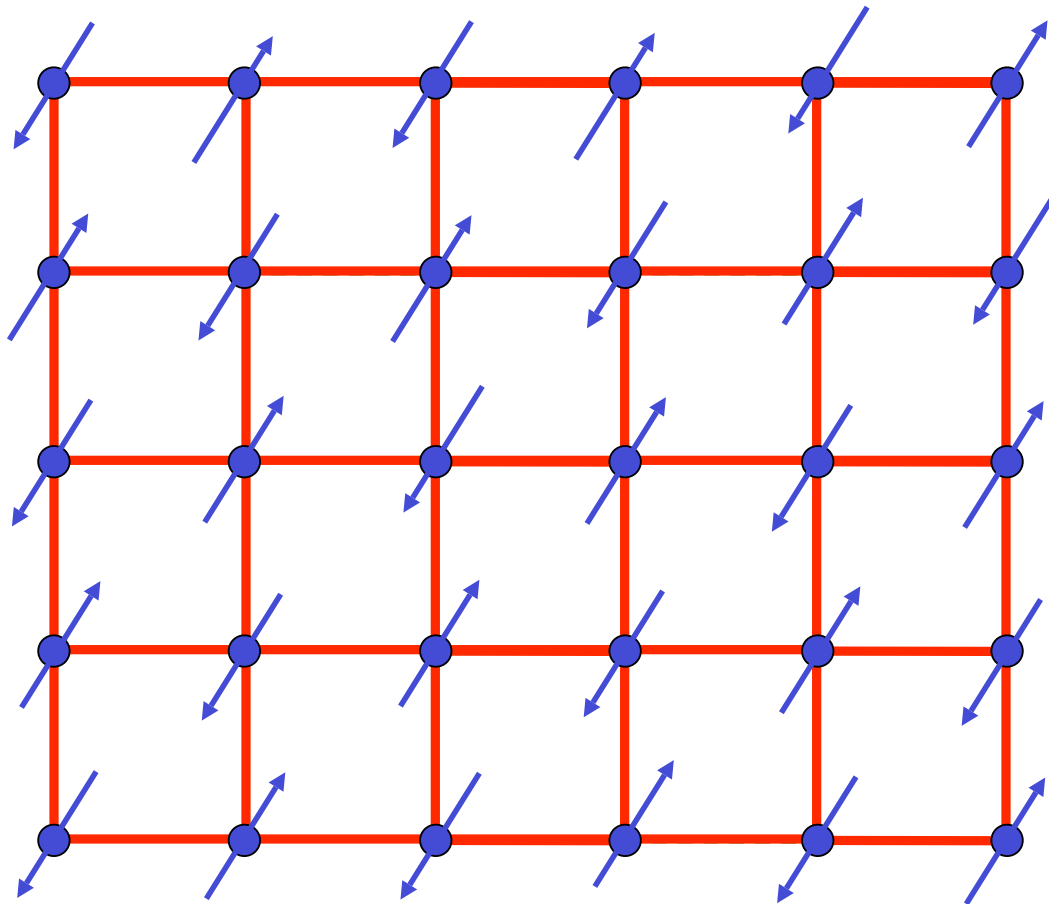
4. Quantum criticality in graphene

Hydrodynamic cyclotron resonance and Nernst effect

The cuprate superconductors

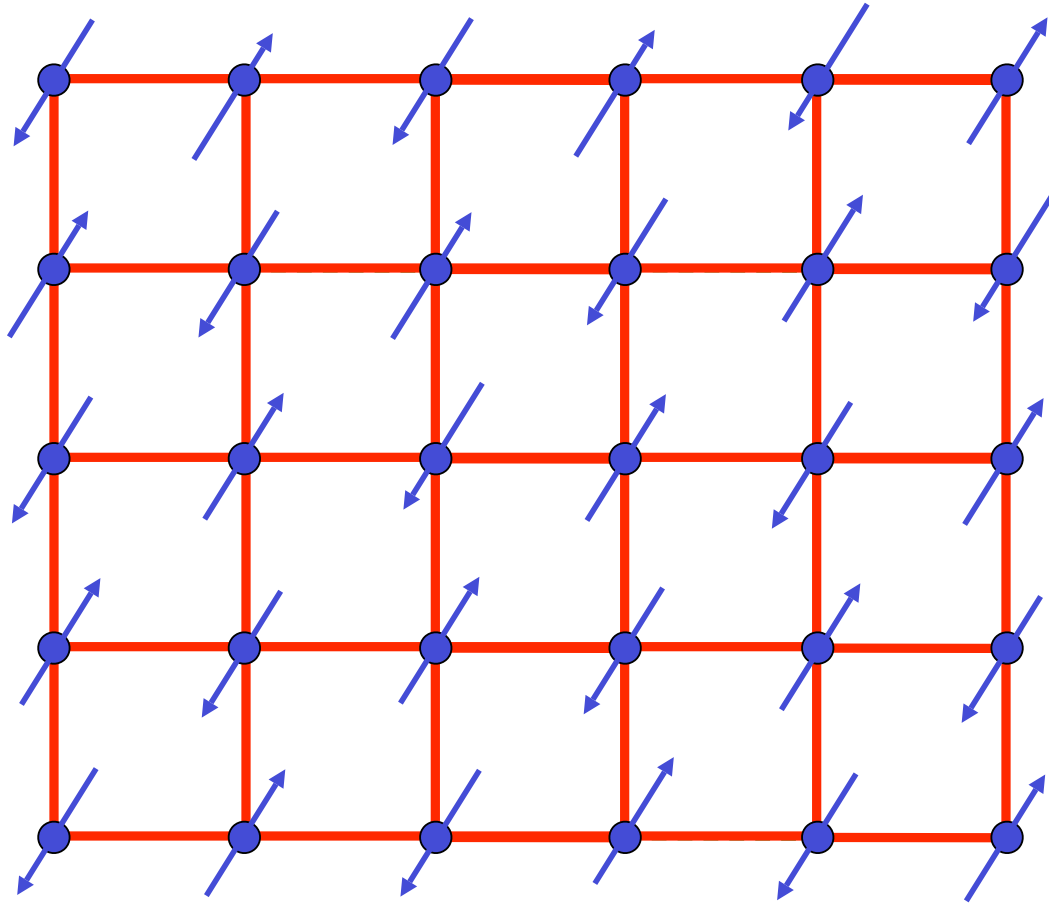


Antiferromagnetic (Neel) order in the insulator

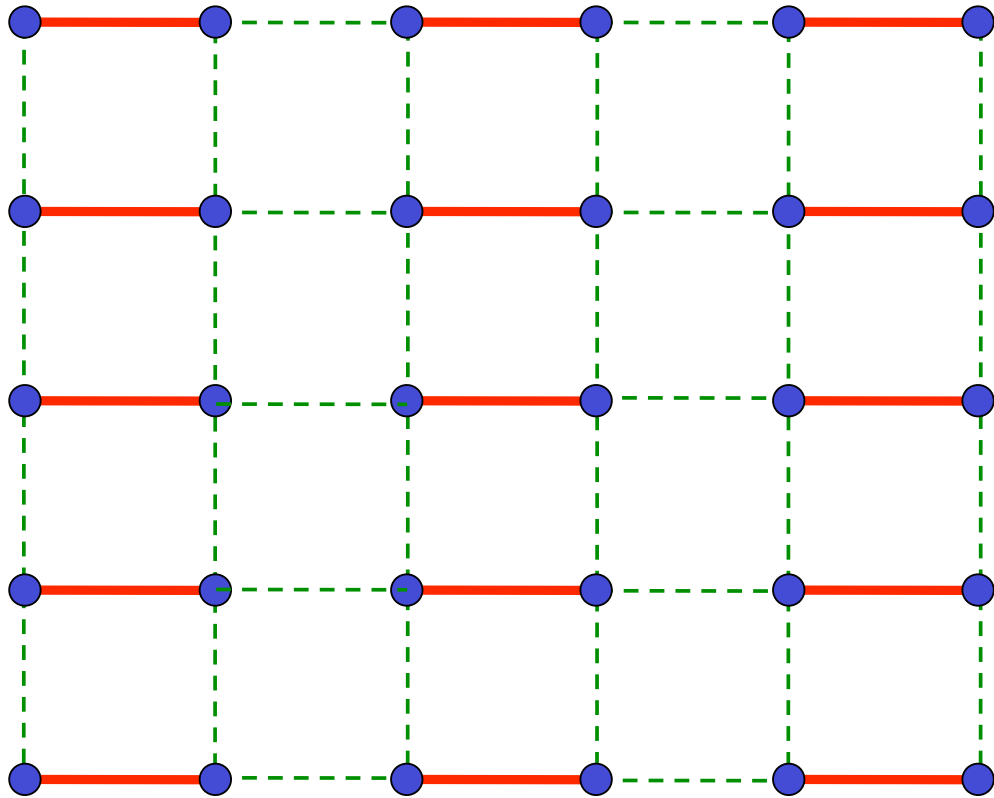


No entanglement of spins

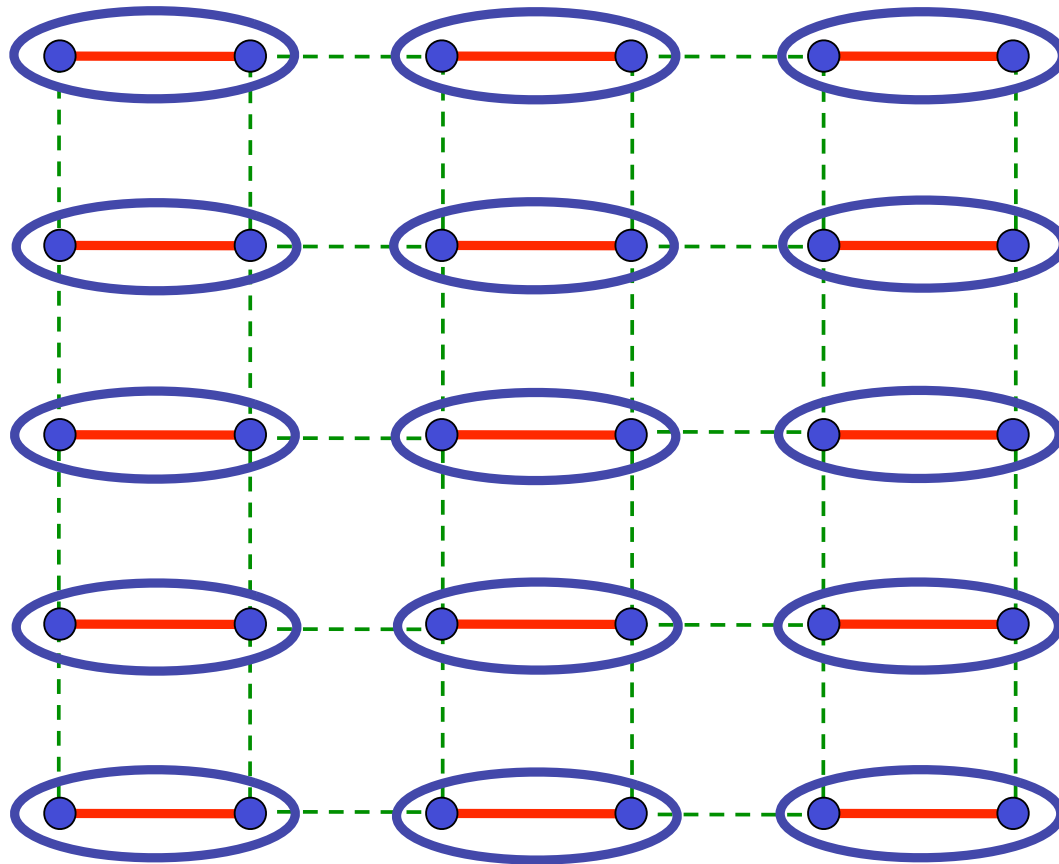
Antiferromagnetic (Neel) order in the insulator




Excitations: 2 spin waves (Goldstone modes)

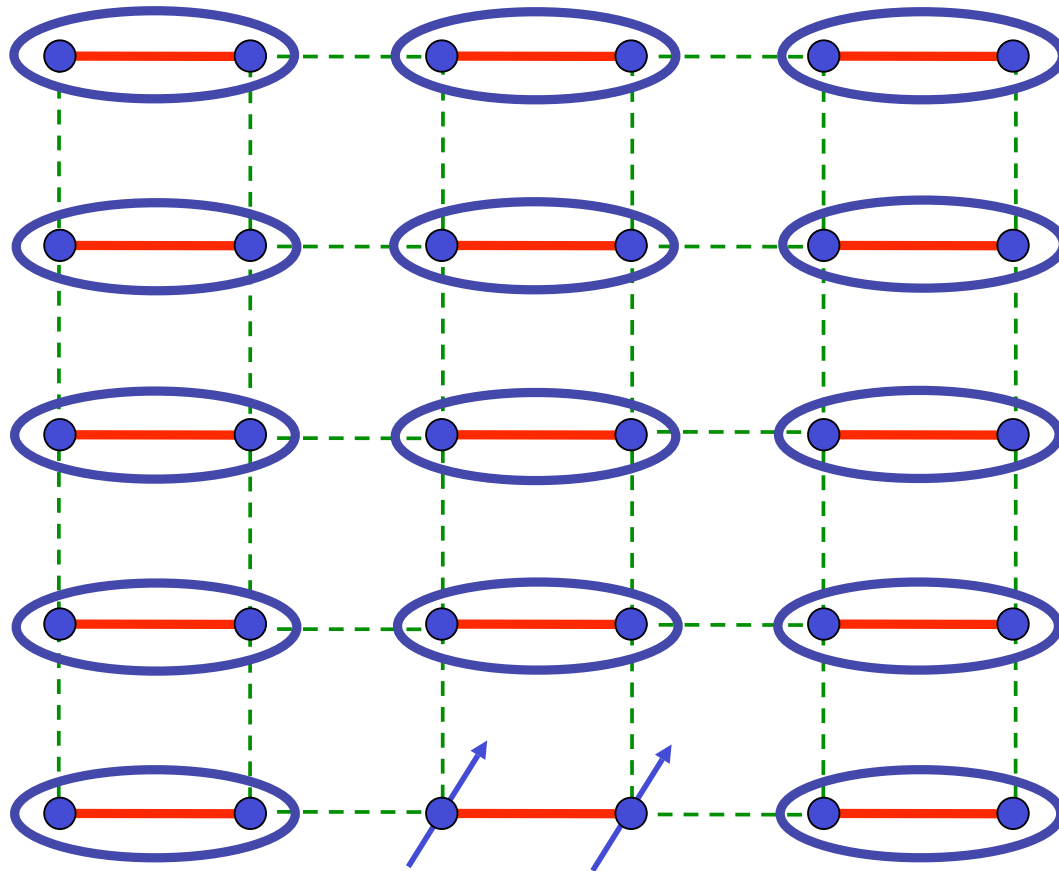


Weaken some bonds to induce spin entanglement in a new quantum phase



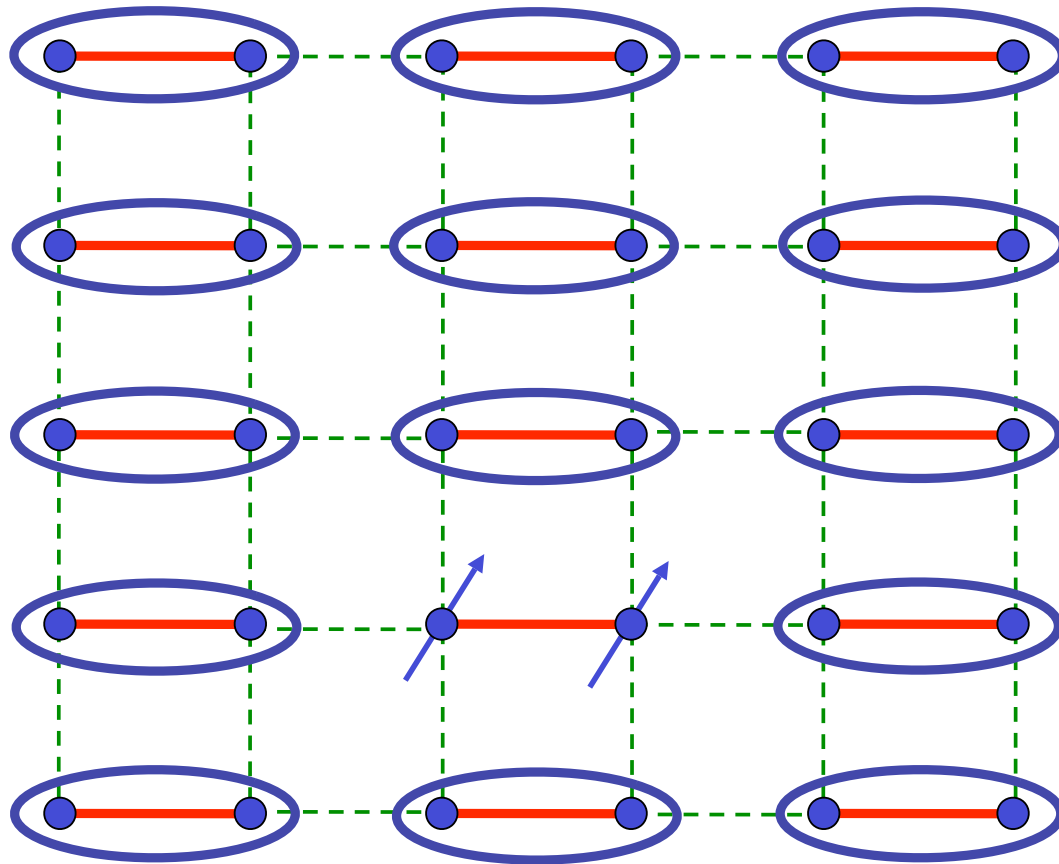

$$= \frac{1}{\sqrt{2}} (|\uparrow\downarrow\rangle - |\downarrow\uparrow\rangle)$$

Ground state is a product of pairs
of entangled spins.



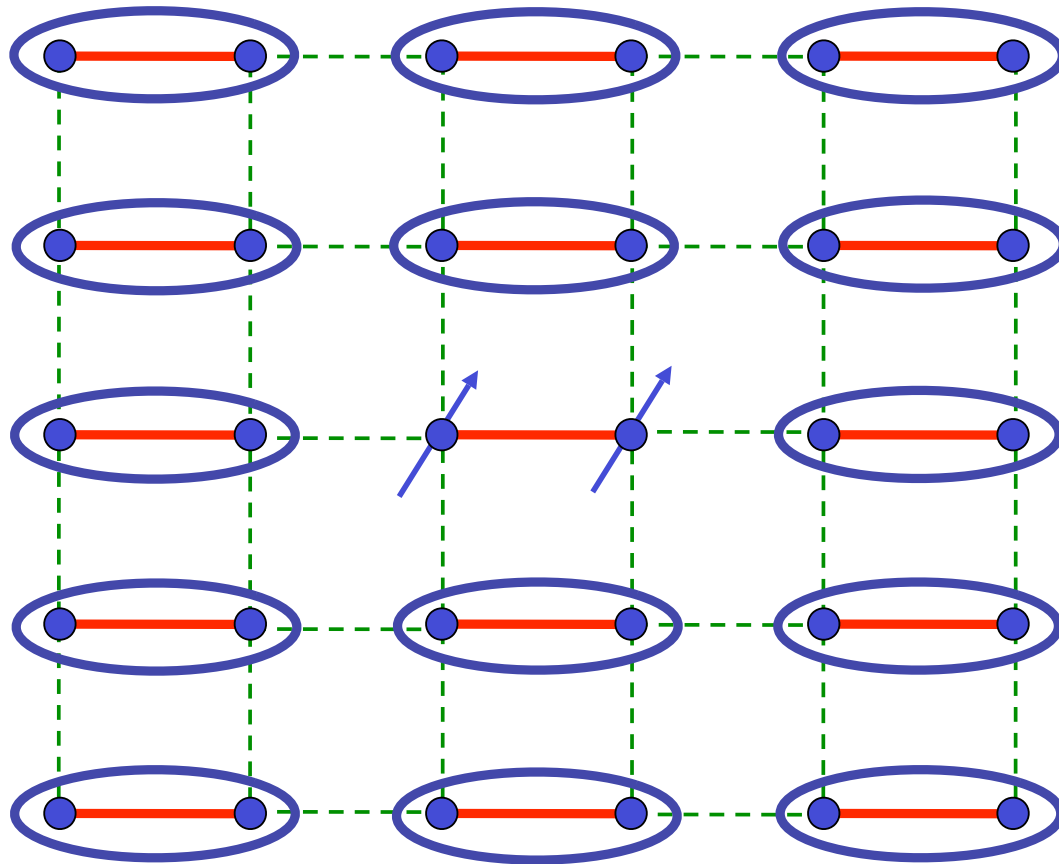
$$\begin{aligned}
 & \text{Diagram of a site with two blue dots in a blue oval} \\
 & = \frac{1}{\sqrt{2}} (|\uparrow\downarrow\rangle - |\downarrow\uparrow\rangle)
 \end{aligned}$$

Excitations: 3 $S=1$ triplons



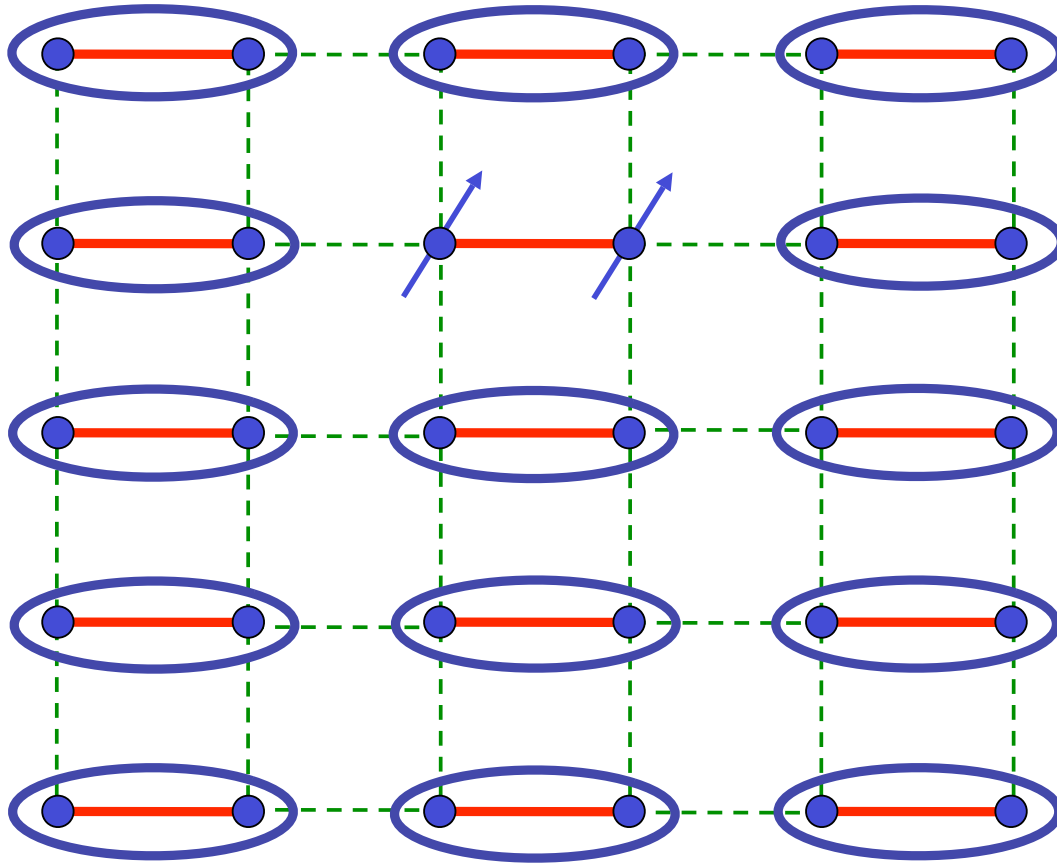
$$= \frac{1}{\sqrt{2}} (|\uparrow\downarrow\rangle - |\downarrow\uparrow\rangle)$$

Excitations: 3 $S=1$ triplons



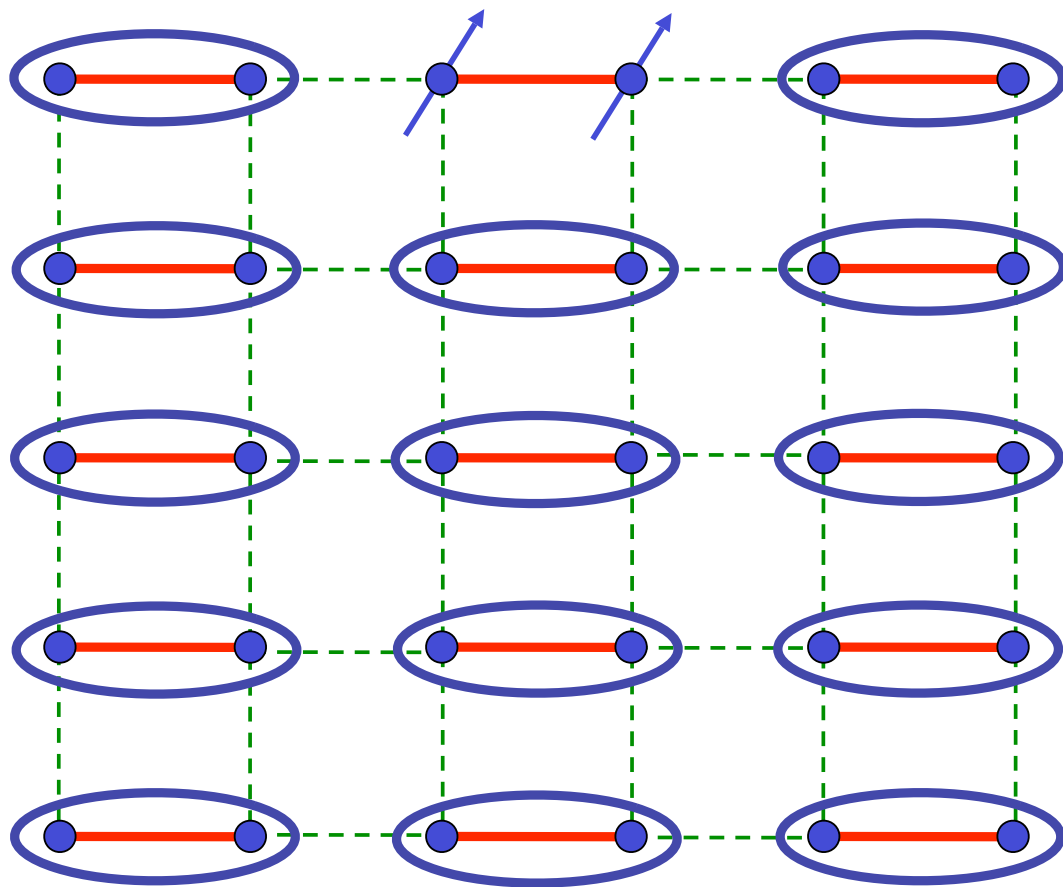
$$= \frac{1}{\sqrt{2}} (|\uparrow\downarrow\rangle - |\downarrow\uparrow\rangle)$$

Excitations: 3 $S=1$ triplons



$$= \frac{1}{\sqrt{2}} (|\uparrow\downarrow\rangle - |\downarrow\uparrow\rangle)$$

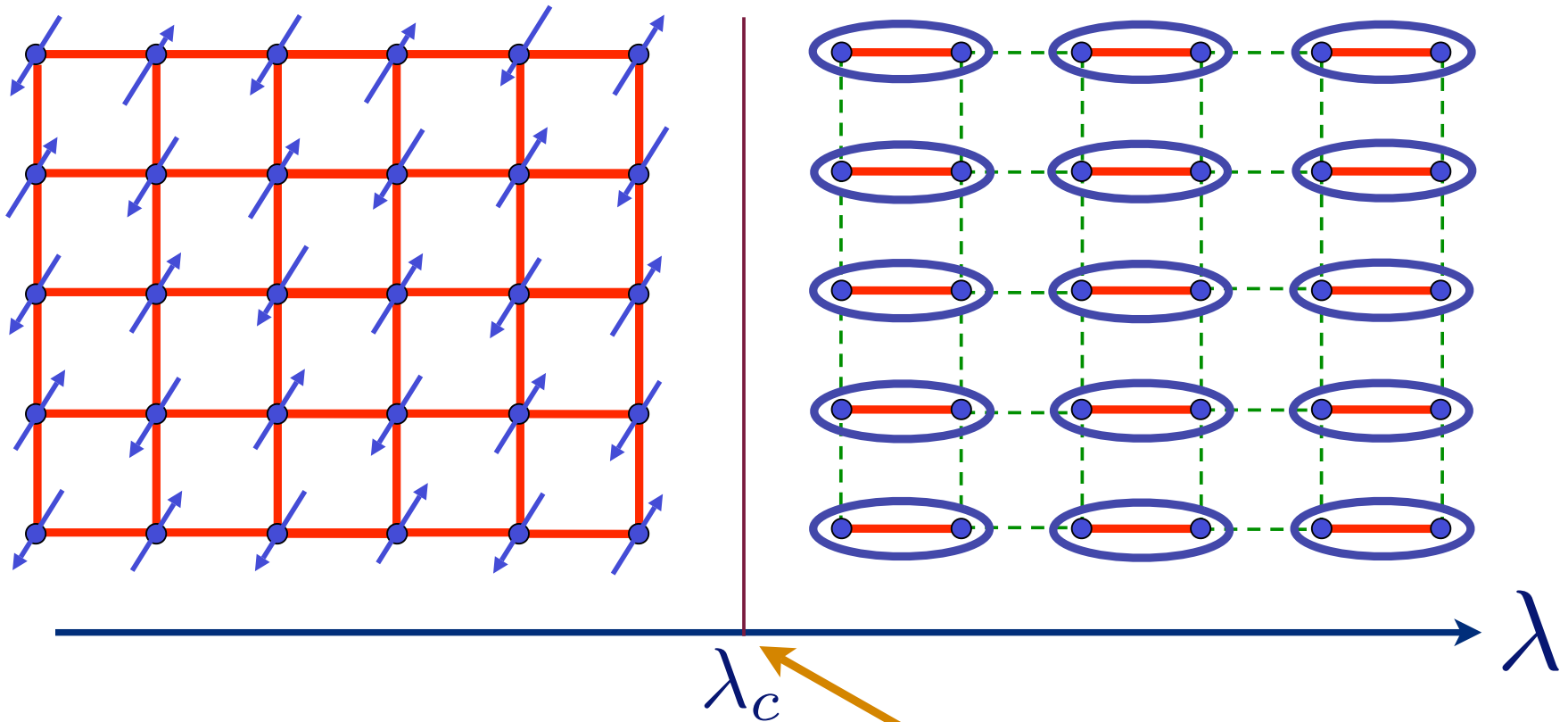
Excitations: 3 $S=1$ triplons



$$= \frac{1}{\sqrt{2}} (|\uparrow\downarrow\rangle - |\downarrow\uparrow\rangle)$$

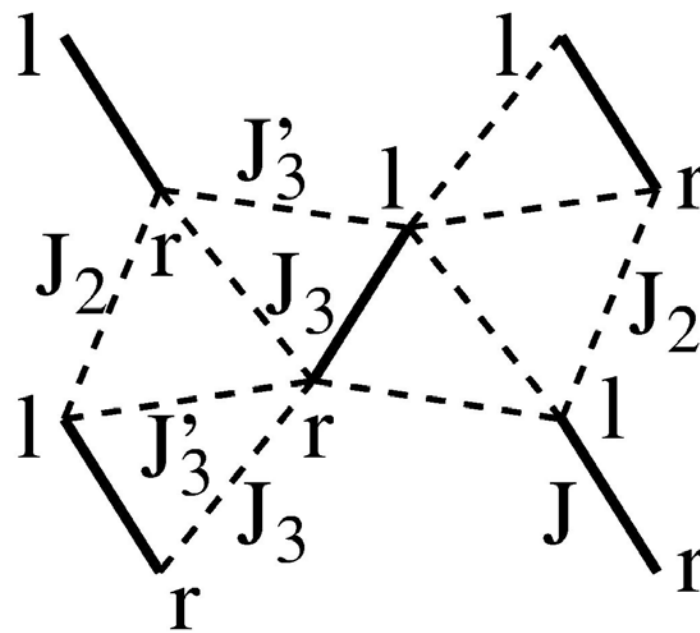
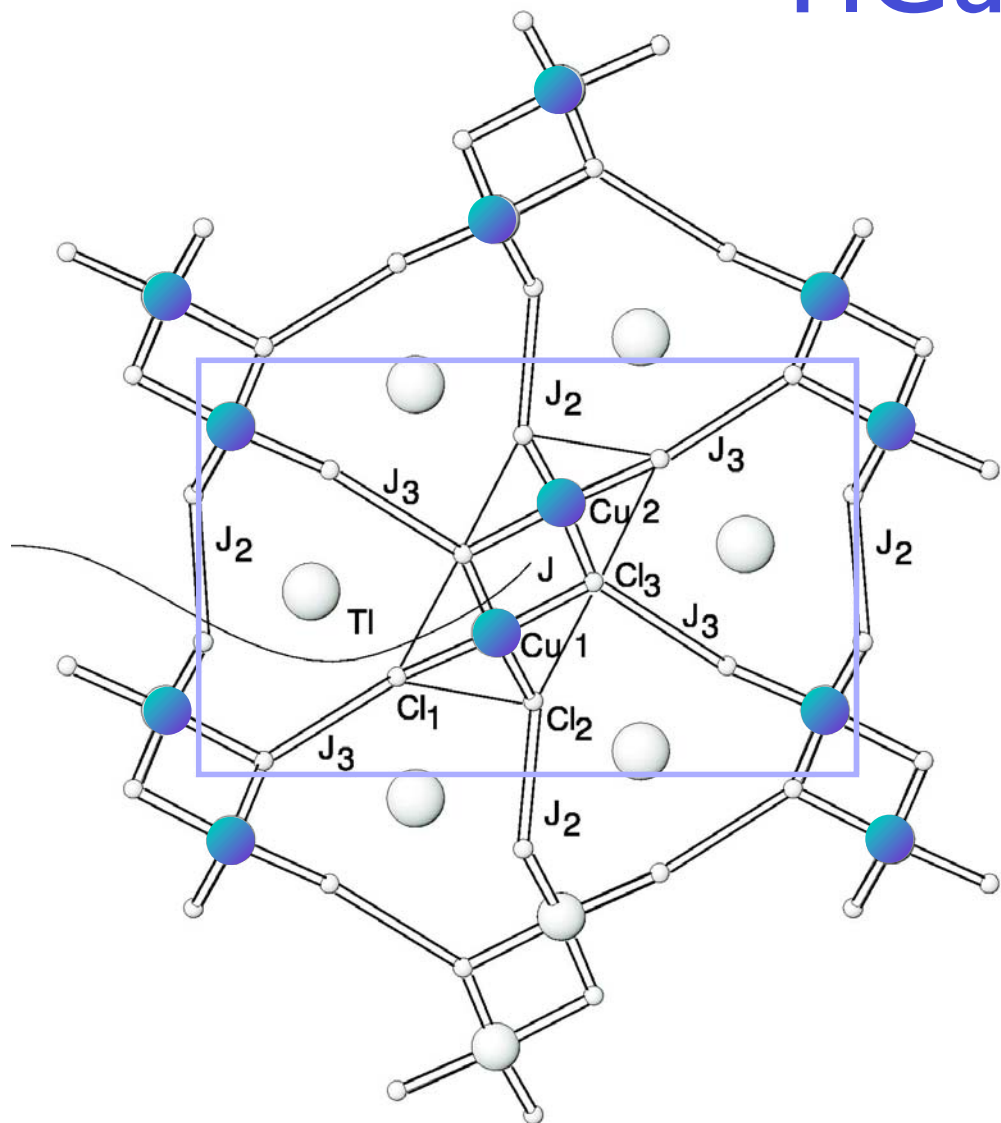
Excitations: 3 $S=1$ triplons

Phase diagram as a function of the ratio of exchange interactions, λ

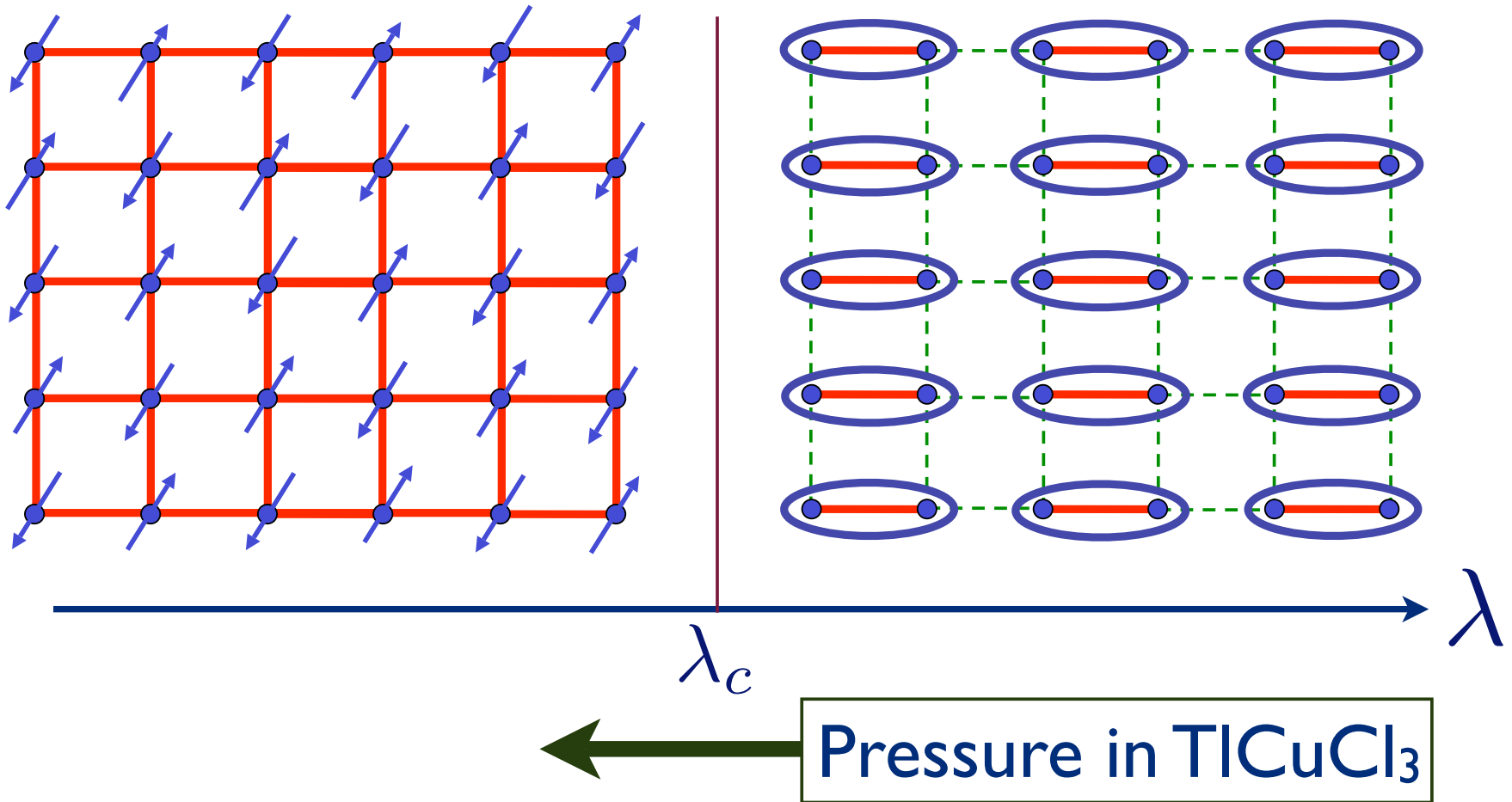


Quantum critical point with non-local entanglement in spin wavefunction

TiCuCl₃



Phase diagram as a function of the ratio of exchange interactions, λ



TlCuCl₃ at ambient pressure

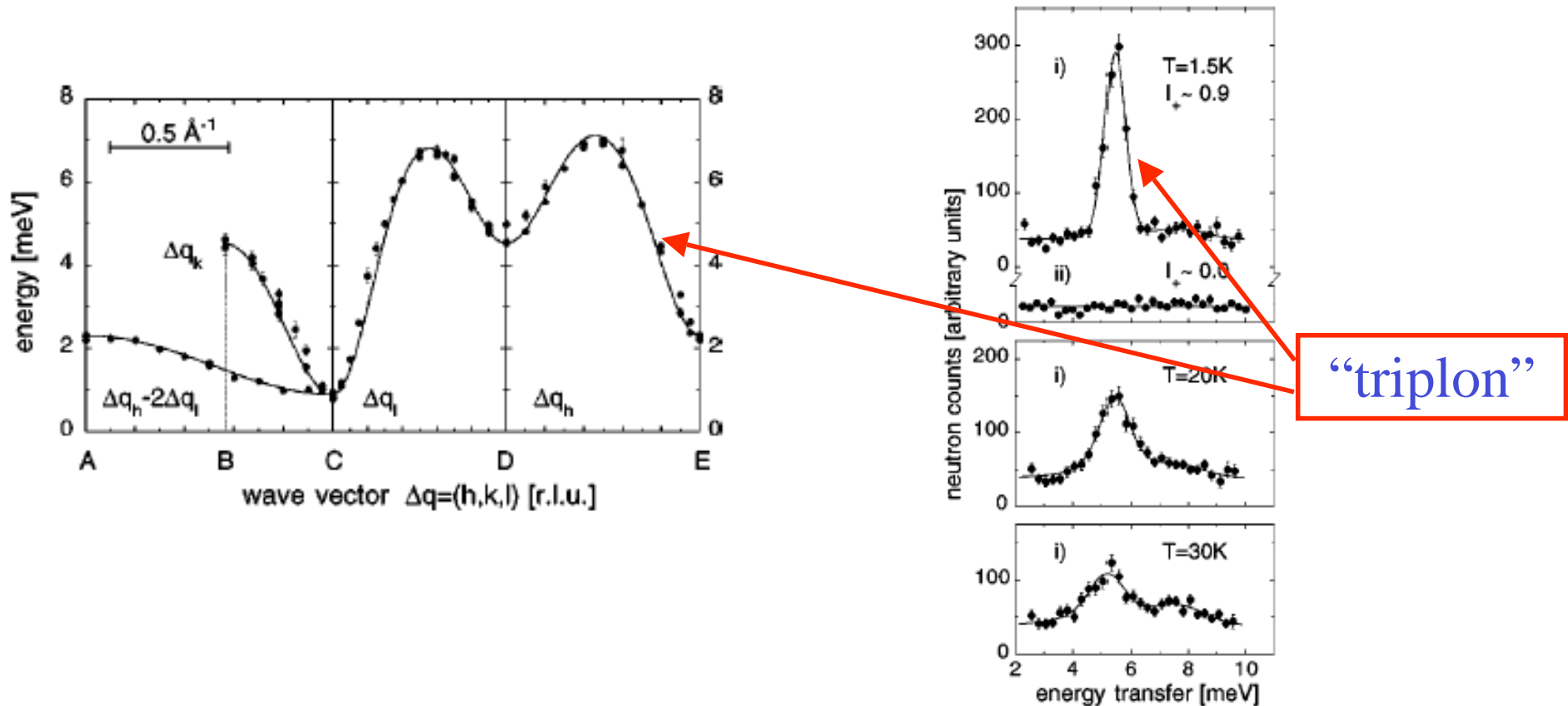
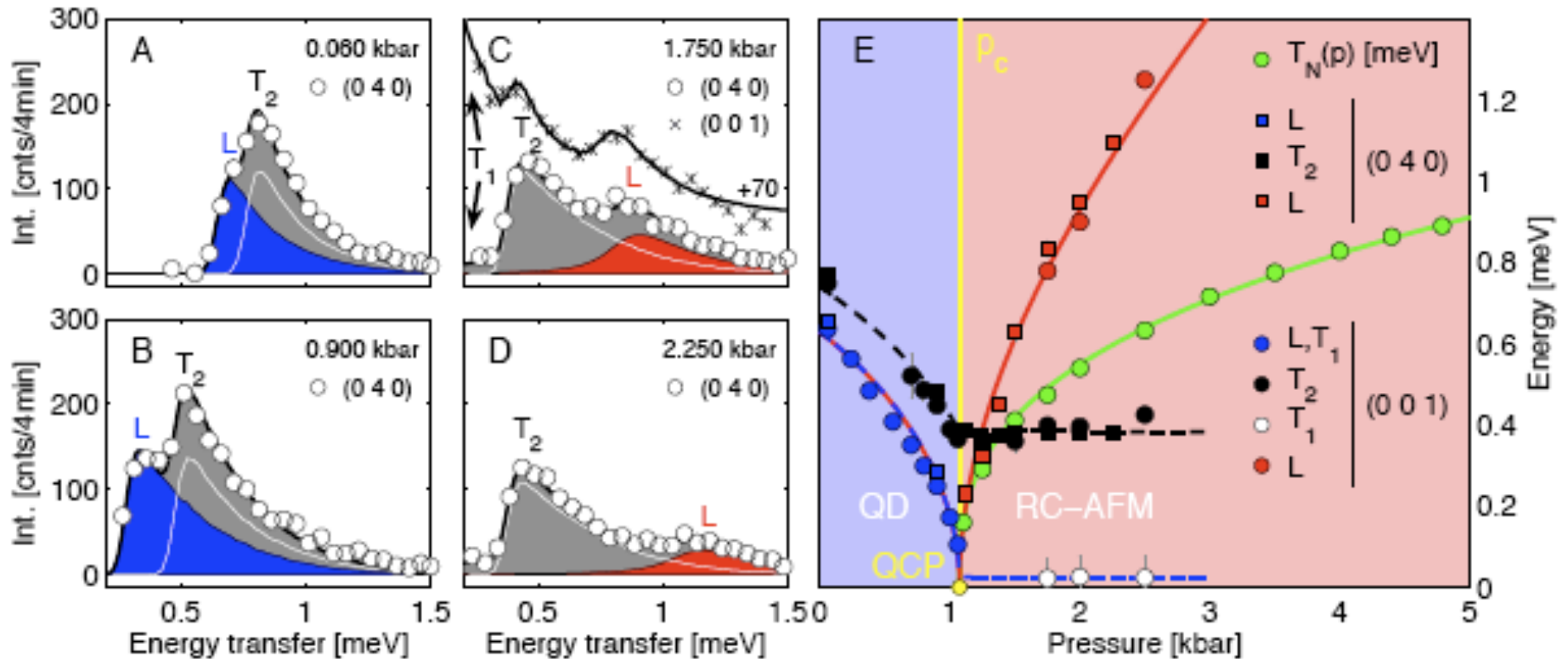


FIG. 1. Measured neutron profiles in the a^*c^* plane of TlCuCl₃ for $i=(1.35,0,0)$, $ii=(0,0,3.15)$ [r.l.u.]. The spectrum at $T=1.5\text{K}$

N. Cavadini, G. Heigold, W. Henggeler, A. Furrer, H.-U. Güdel, K. Krämer and H. Mutka, *Phys. Rev. B* 63 172414 (2001).

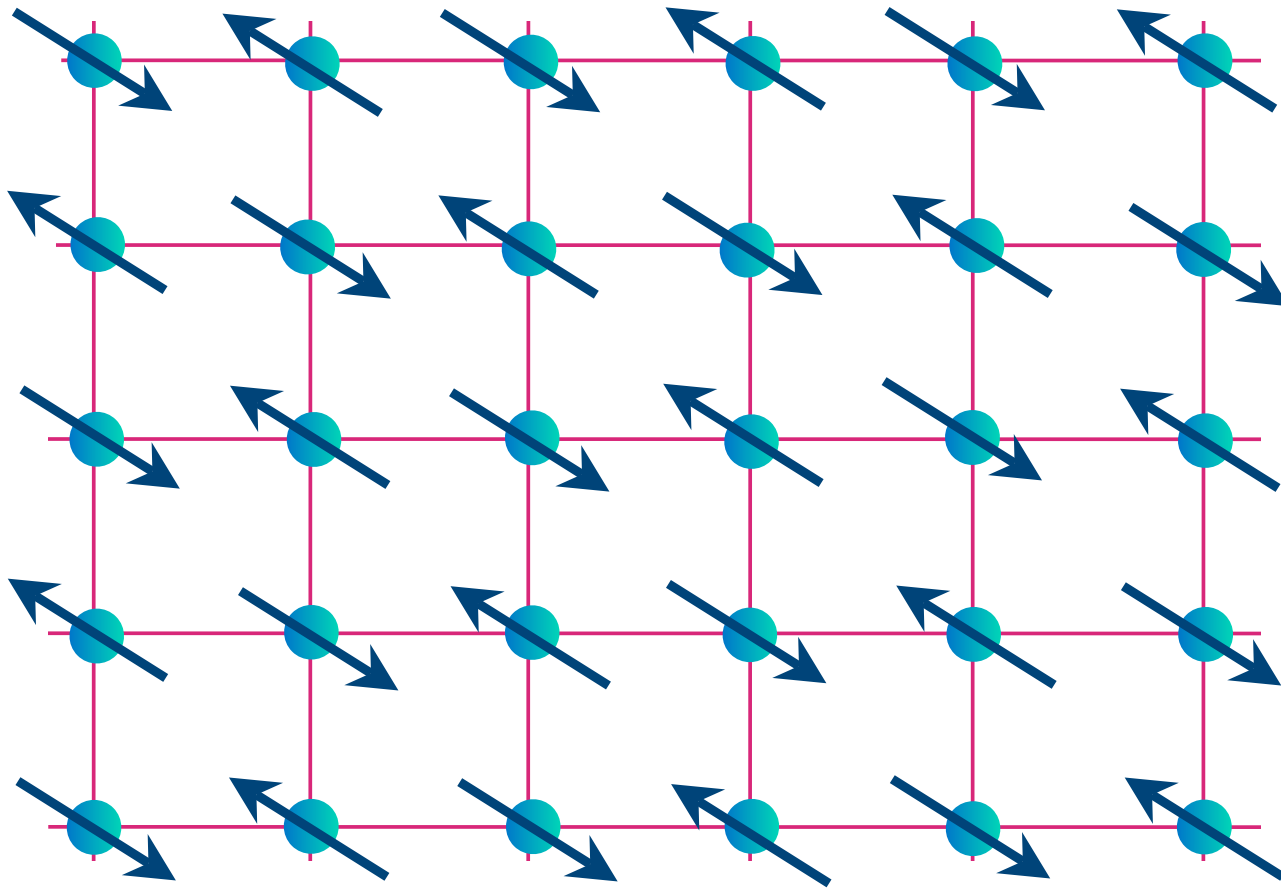
TiCuCl₃ with varying pressure



Observation of 3 → 2 low energy modes, emergence of new longitudinal mode in Néel phase, and vanishing of Néel temperature at the quantum critical point

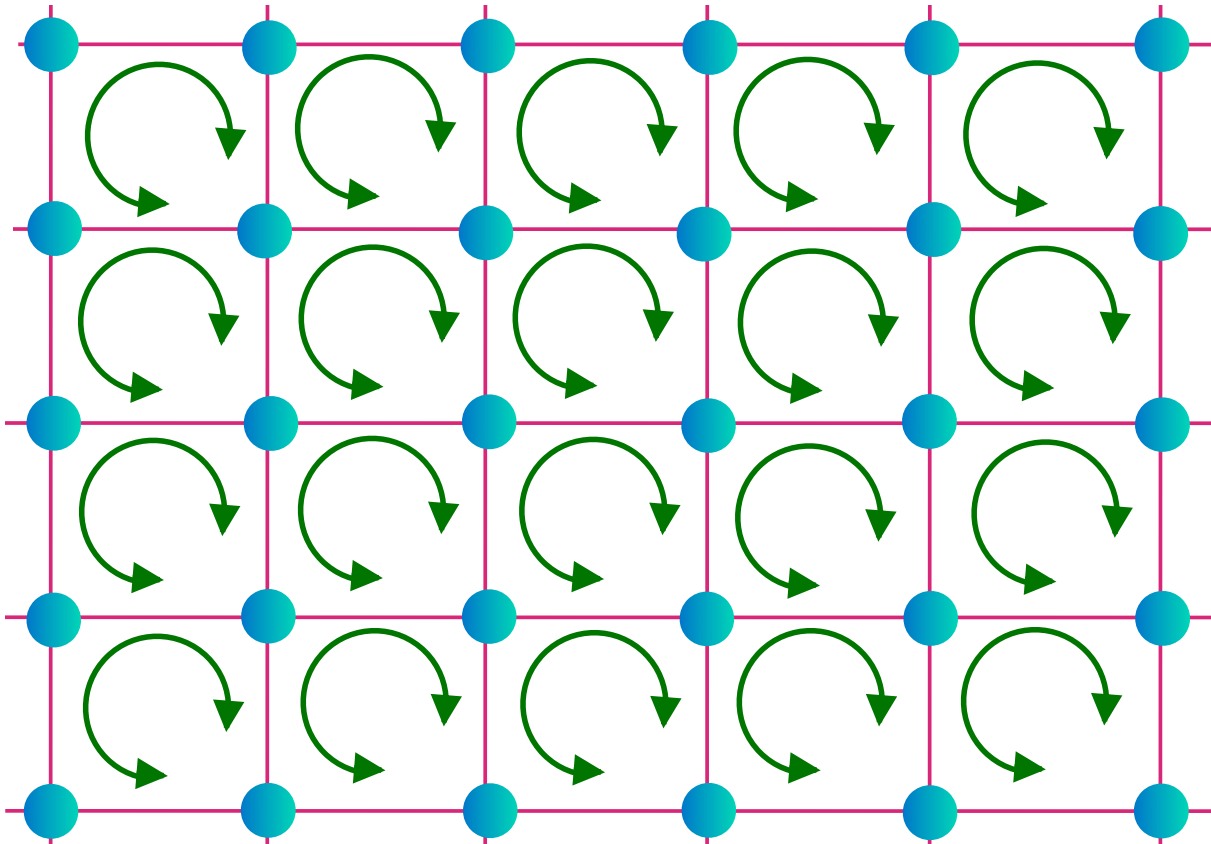
Christian Ruedg, Bruce Normand, Masashige Matsumoto, Albert Furrer, Desmond McMorrow, Karl Kramer, Hans-Ulrich Gudel, Severian Gvasaliya, Hannu Mutka, and Martin Boehm, arXiv:0803.3720

Quantum phase transition with full square lattice symmetry



$$H = J \sum_{\langle ij \rangle} \vec{S}_i \cdot \vec{S}_j ; \vec{S}_i \Rightarrow \text{spin operator with } S = 1/2$$

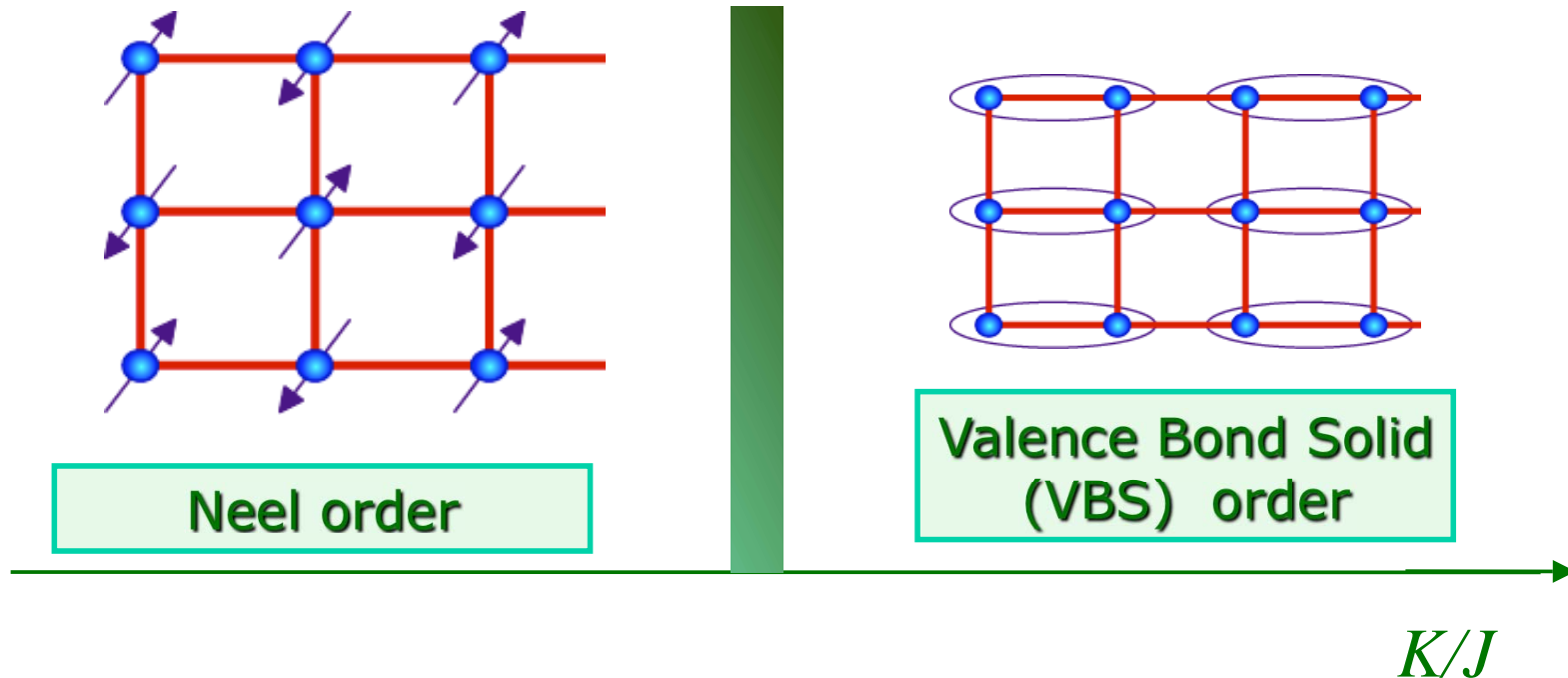
Quantum phase transition with full square lattice symmetry



$$H = J \sum_{\langle ij \rangle} \vec{S}_i \cdot \vec{S}_j + K \sum_{\square} \text{four spin exchange}$$

A. W. Sandvik, *Phys. Rev. Lett.* **98**, 227202 (2007)

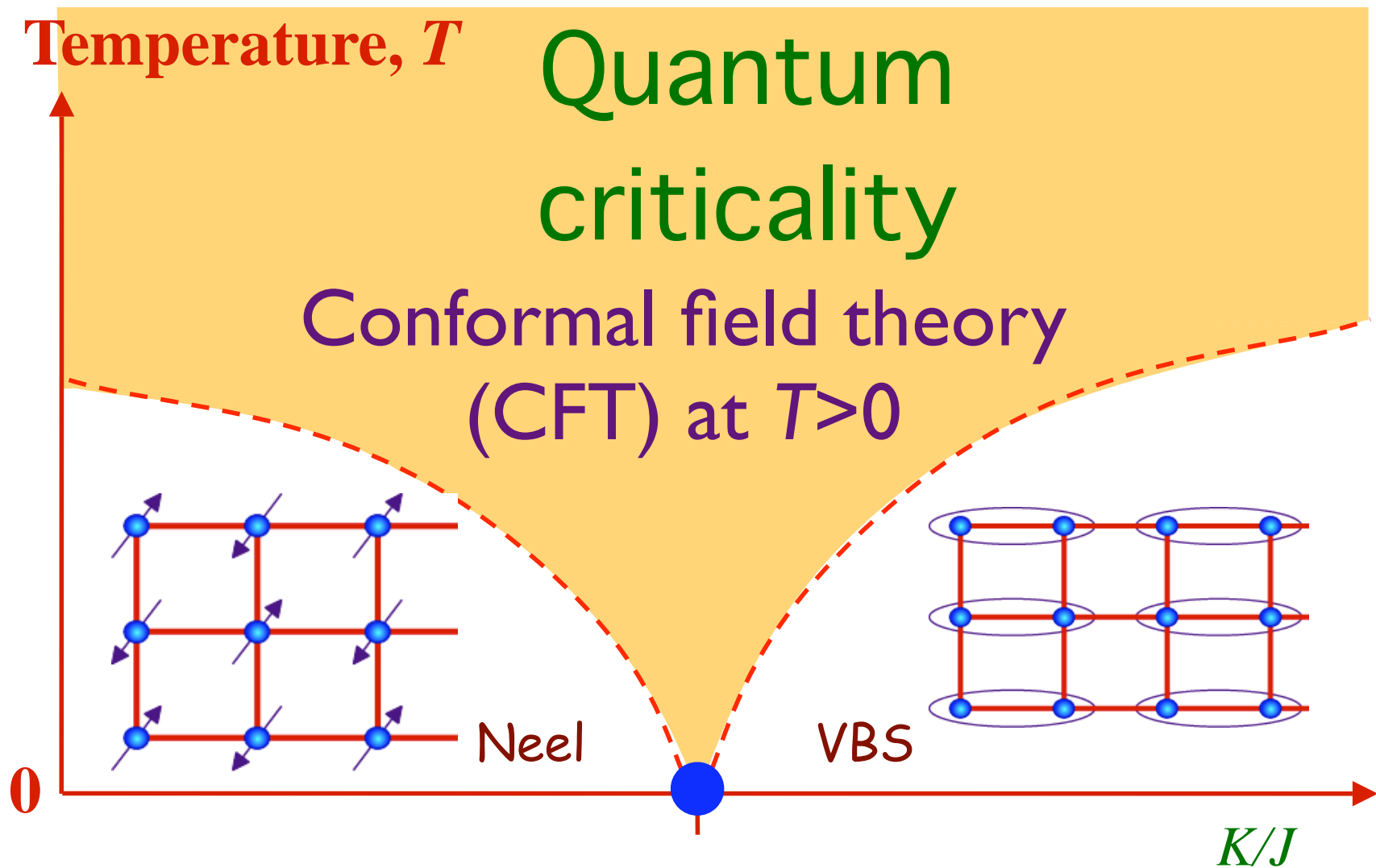
Quantum phase transition with full square lattice symmetry



$$H = J \sum_{\langle ij \rangle} \vec{S}_i \cdot \vec{S}_j + K \sum_{\square} \text{four spin exchange}$$

A. W. Sandvik, *Phys. Rev. Lett.* **98**, 227202 (2007)
 N. Read and S. Sachdev, *Phys. Rev. Lett.* **62**, 1694 (1989).

Why should we care about the entanglement at an isolated critical point in the parameter space ?



Outline

1. Entanglement of spins

Experiments on antiferromagnetic insulators

2. Black Hole Thermodynamics

Connections to quantum criticality

3. Nernst effect in the cuprate superconductors

Quantum criticality and dyonic black holes

4. Quantum criticality in graphene

Hydrodynamic cyclotron resonance and Nernst effect

Outline

1. Entanglement of spins

Experiments on antiferromagnetic insulators

2. Black Hole Thermodynamics

Connections to quantum criticality

3. Nernst effect in the cuprate superconductors

Quantum criticality and dyonic black holes

4. Quantum criticality in graphene

Hydrodynamic cyclotron resonance and Nernst effect

Black Holes

Objects so massive that light is gravitationally bound to them.

Black Holes

Objects so massive that light is gravitationally bound to them.

The region inside the black hole **horizon** is causally disconnected from the rest of the universe.

$$\text{Horizon radius } R = \frac{2GM}{c^2}$$

Black Hole Thermodynamics

Bekenstein and Hawking discovered astonishing connections between the Einstein theory of black holes and the laws of thermodynamics

$$\text{Entropy of a black hole } S = \frac{k_B A}{4\ell_P^2}$$

where A is the area of the horizon, and

$$\ell_P = \sqrt{\frac{G\hbar}{c^3}} \text{ is the Planck length.}$$

The Second Law: $dA \geq 0$

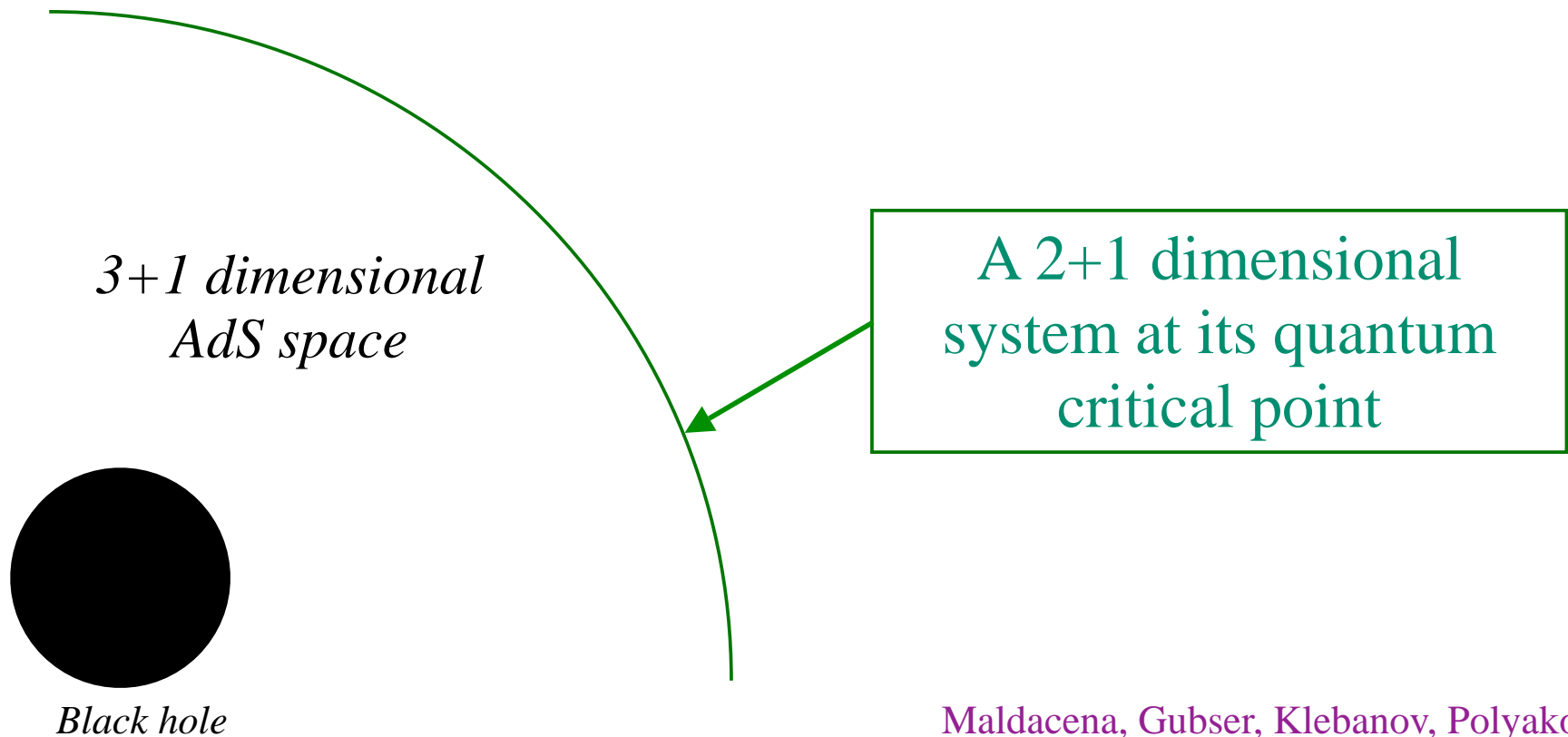
Black Hole Thermodynamics

Bekenstein and Hawking discovered astonishing connections between the Einstein theory of black holes and the laws of thermodynamics

Horizon temperature: $4\pi k_B T = \frac{\hbar^2}{2M\ell_P^2}$

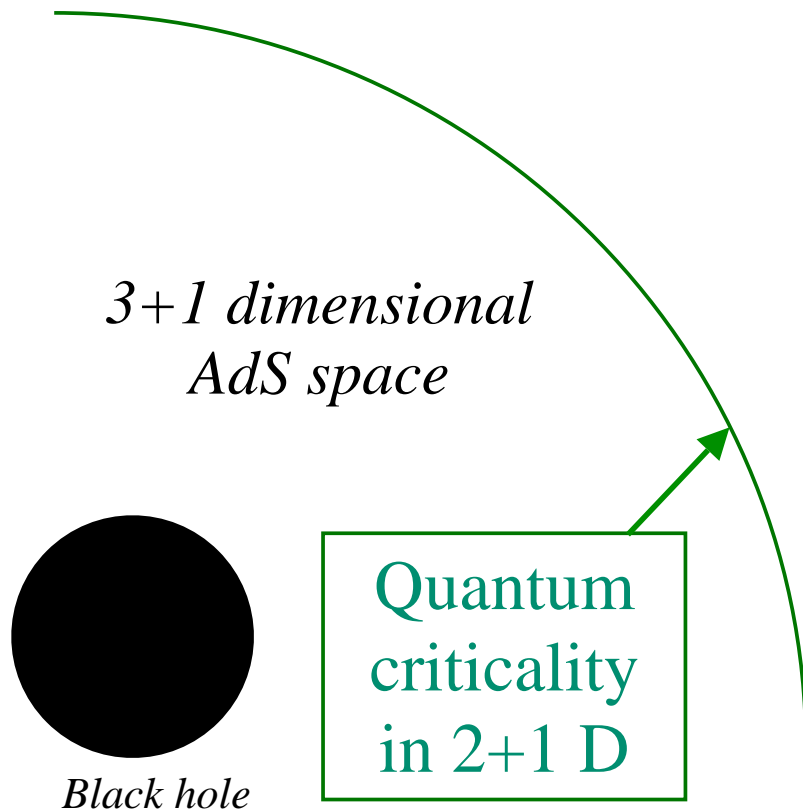
AdS/CFT correspondence

The quantum theory of a black hole in a 3+1-dimensional negatively curved AdS universe is holographically represented by a CFT (the theory of a quantum critical point) in 2+1 dimensions



AdS/CFT correspondence

The quantum theory of a black hole in a 3+1-dimensional negatively curved AdS universe is holographically represented by a CFT (the theory of a quantum critical point) in 2+1 dimensions

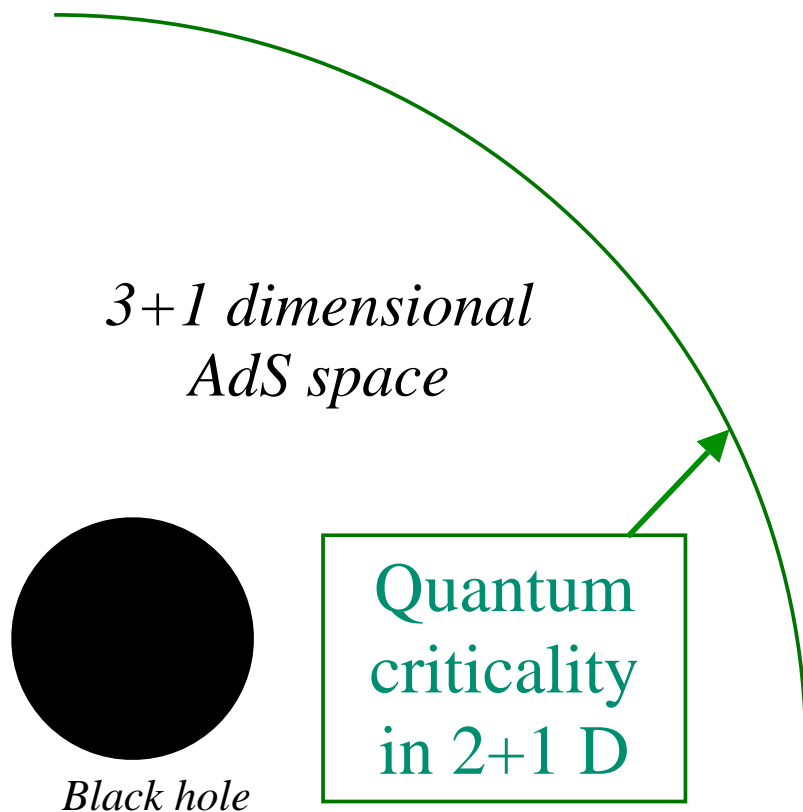


Black hole
temperature =
temperature of
quantum
criticality

Strominger, Vafa

AdS/CFT correspondence

The quantum theory of a black hole in a 3+1-dimensional negatively curved AdS universe is holographically represented by a CFT (the theory of a quantum critical point) in 2+1 dimensions

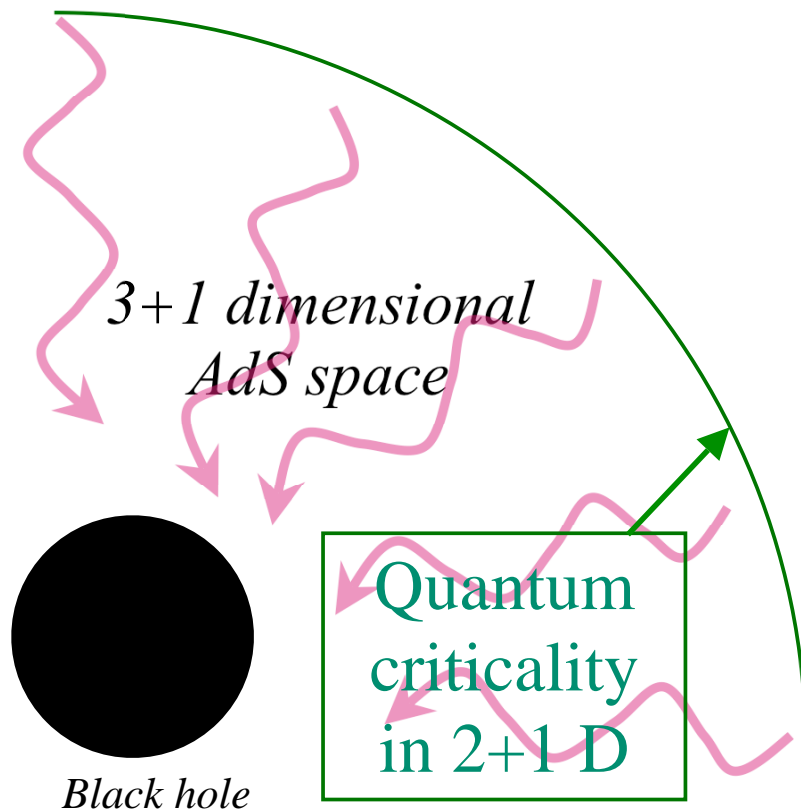


Black hole entropy
= entropy of
quantum criticality
in 2+1 dimensions

Strominger, Vafa

AdS/CFT correspondence

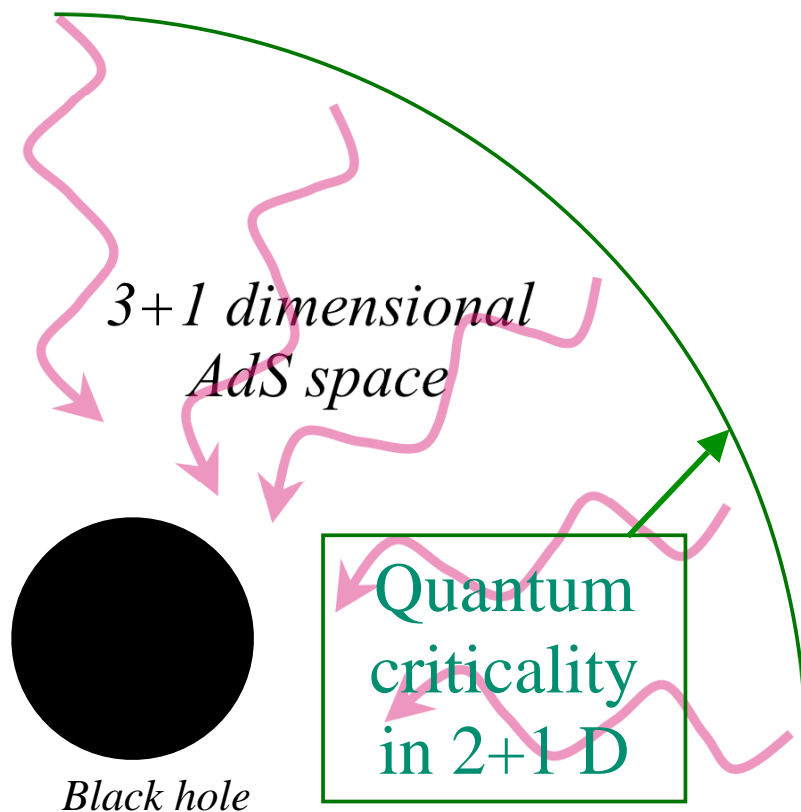
The quantum theory of a black hole in a 3+1-dimensional negatively curved AdS universe is holographically represented by a CFT (the theory of a quantum critical point) in 2+1 dimensions



Dynamics of quantum criticality = waves in curved gravitational background

AdS/CFT correspondence

The quantum theory of a black hole in a 3+1-dimensional negatively curved AdS universe is holographically represented by a CFT (the theory of a quantum critical point) in 2+1 dimensions



“Friction” of quantum critical dynamics = black hole absorption rates

Outline

1. Entanglement of spins

Experiments on antiferromagnetic insulators

2. Black Hole Thermodynamics

Connections to quantum criticality

3. Nernst effect in the cuprate superconductors

Quantum criticality and dyonic black holes

4. Quantum criticality in graphene

Hydrodynamic cyclotron resonance and Nernst effect

Outline

1. Entanglement of spins

Experiments on antiferromagnetic insulators

2. Black Hole Thermodynamics

Connections to quantum criticality

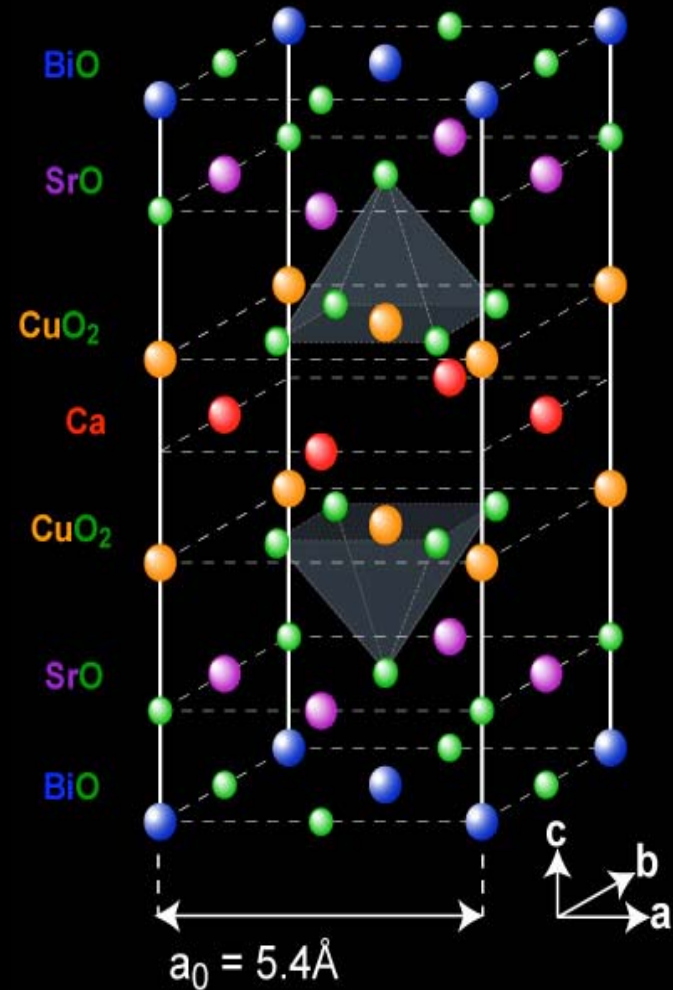
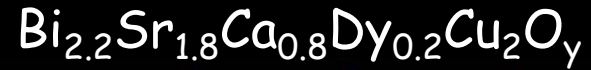
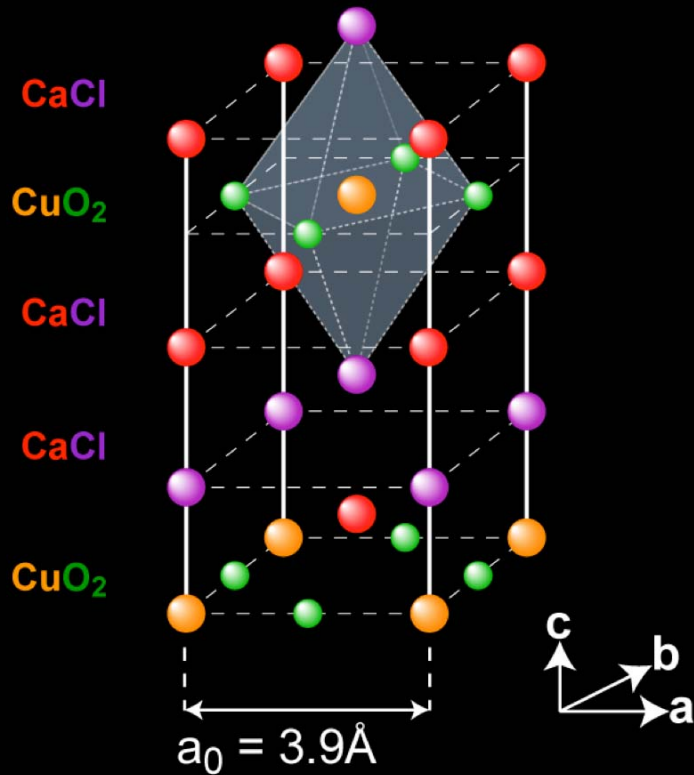
3. Nernst effect in the cuprate superconductors

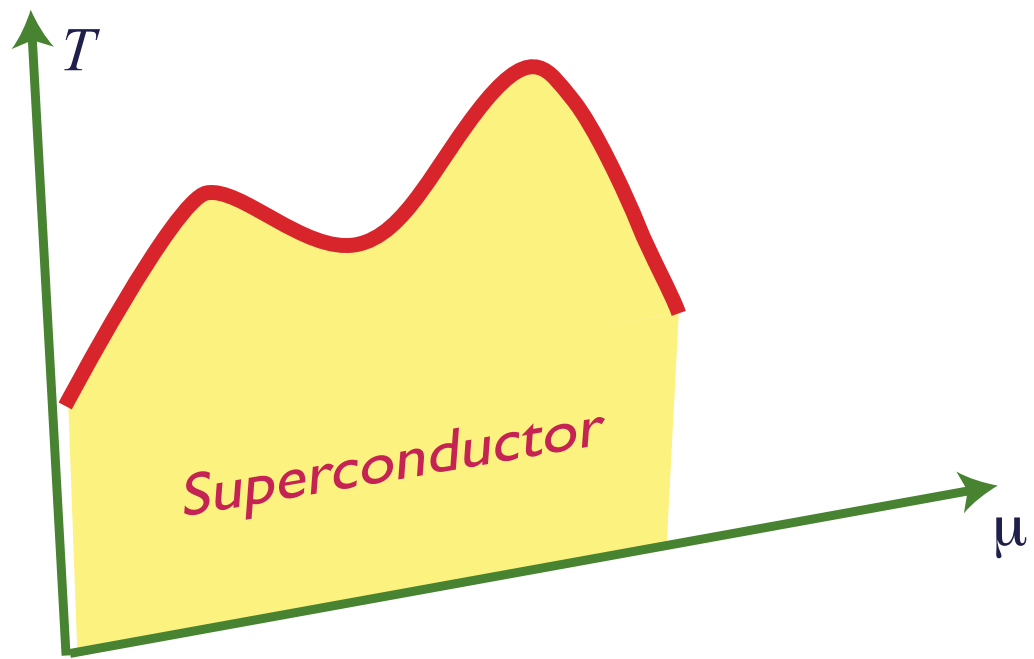
Quantum criticality and dyonic black holes

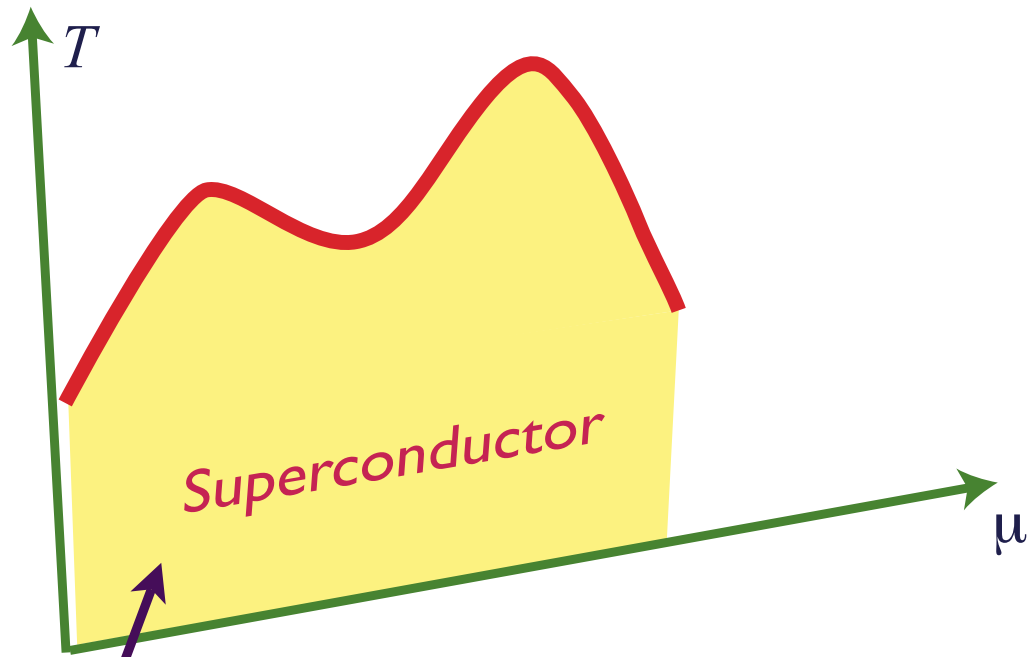
4. Quantum criticality in graphene

Hydrodynamic cyclotron resonance and Nernst effect

Dope the antiferromagnets with charge carriers of density x by applying a chemical potential μ

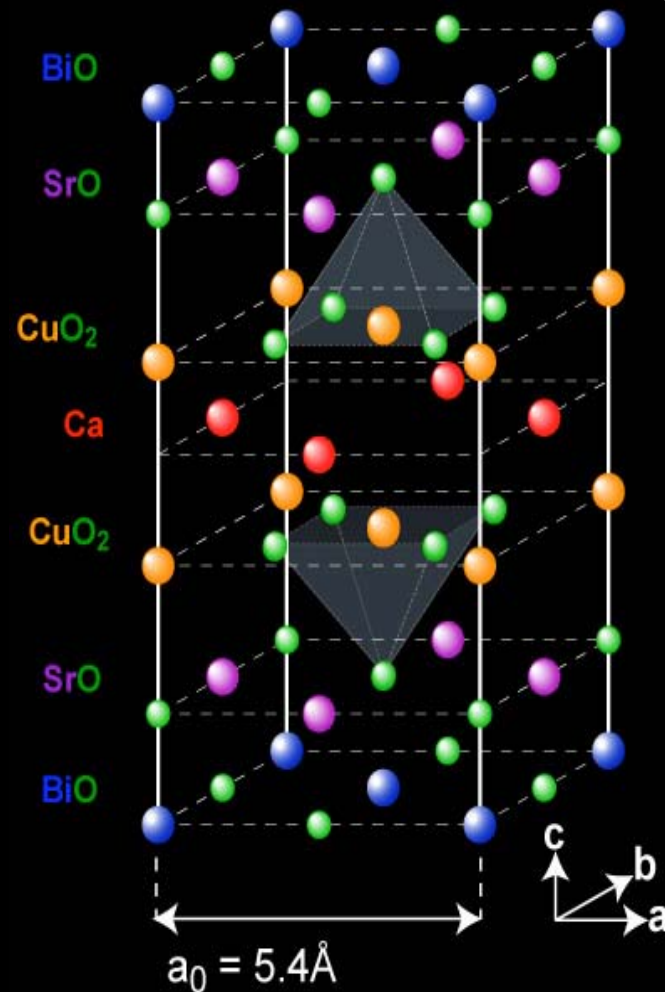
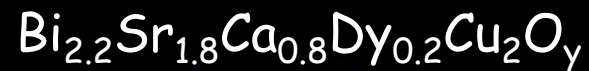
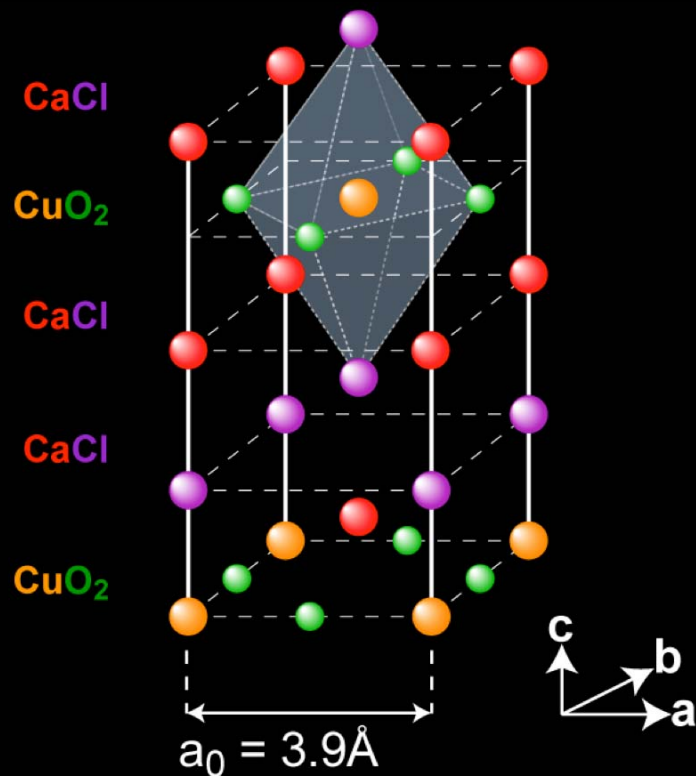
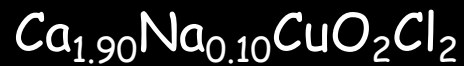




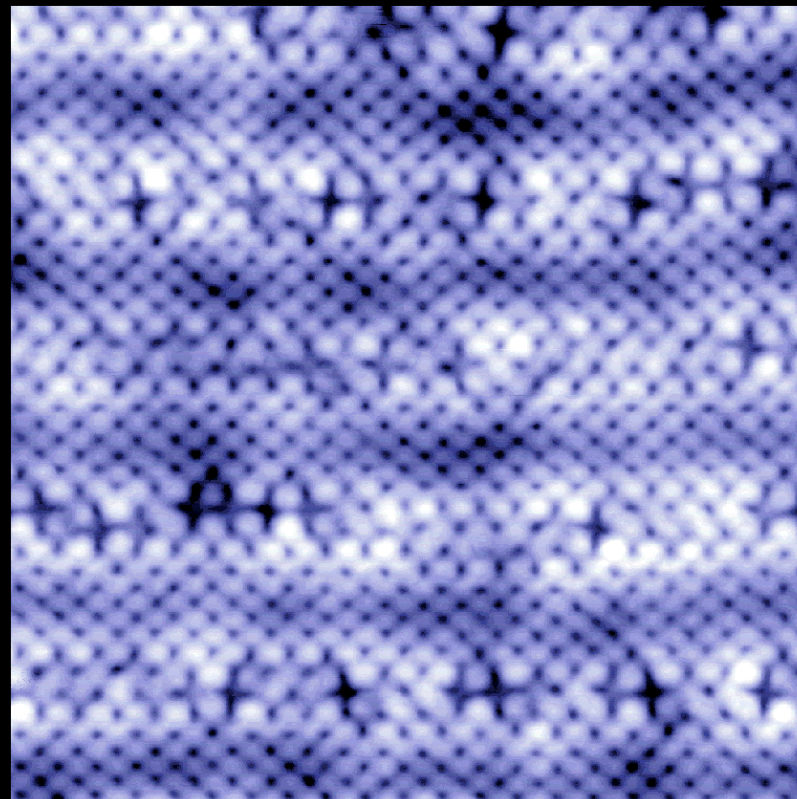
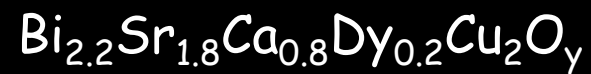
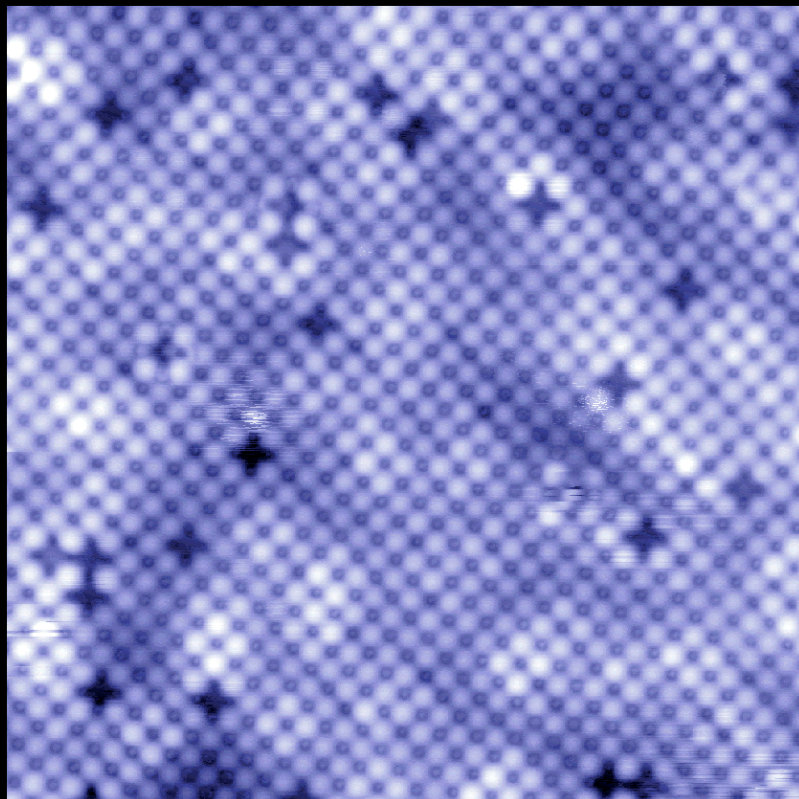
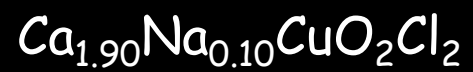


Scanning tunnelling microscopy

STM studies of the underdoped superconductor

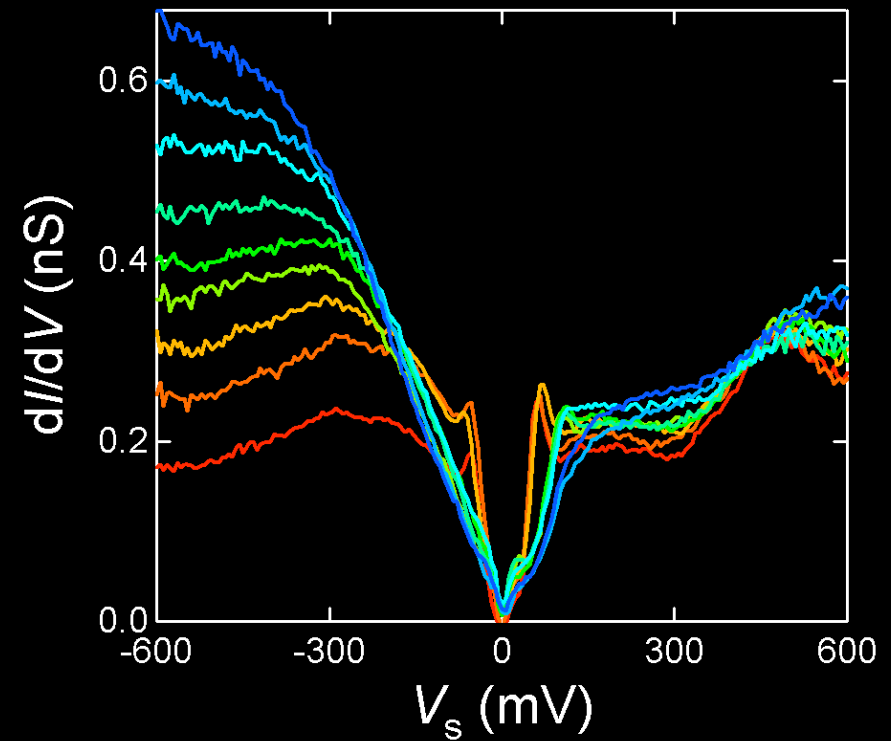
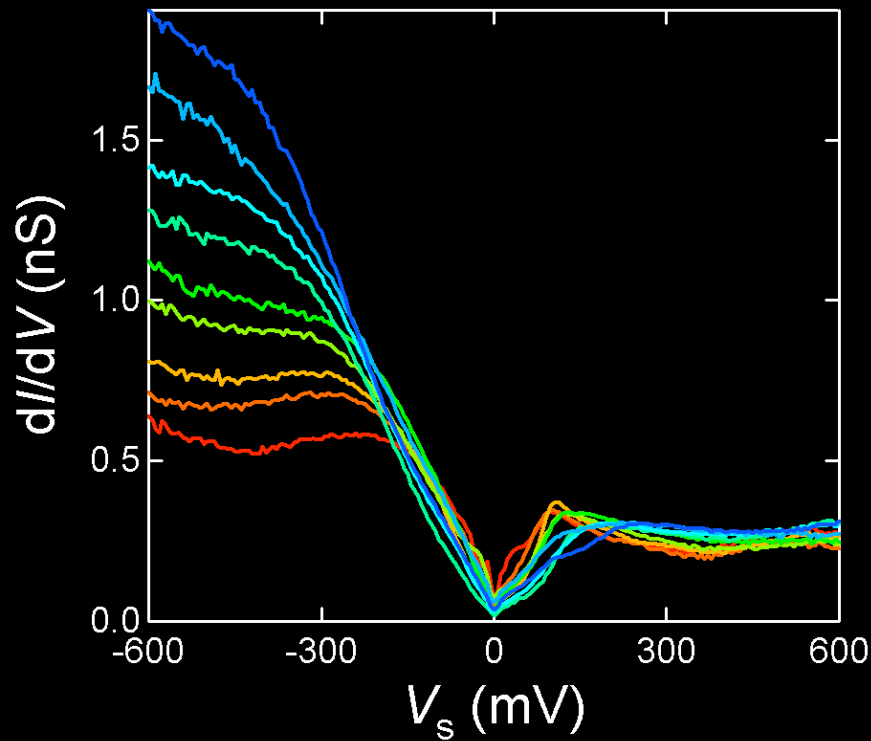
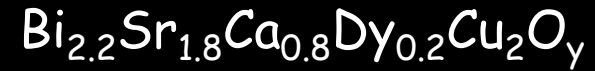
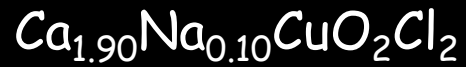


Topograph



12 nm

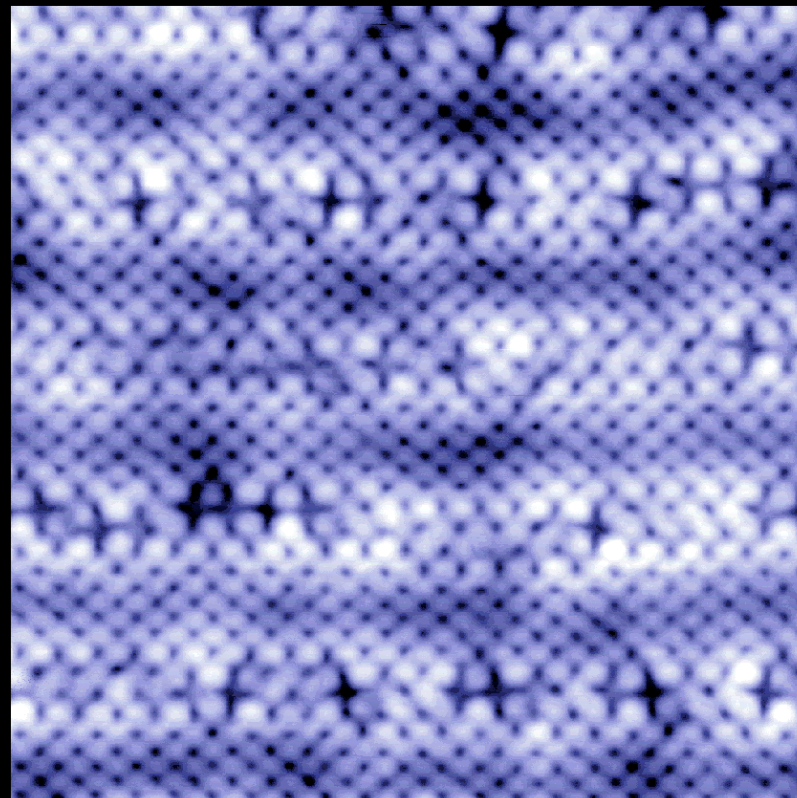
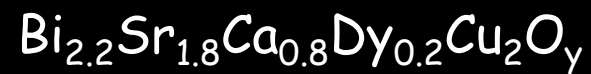
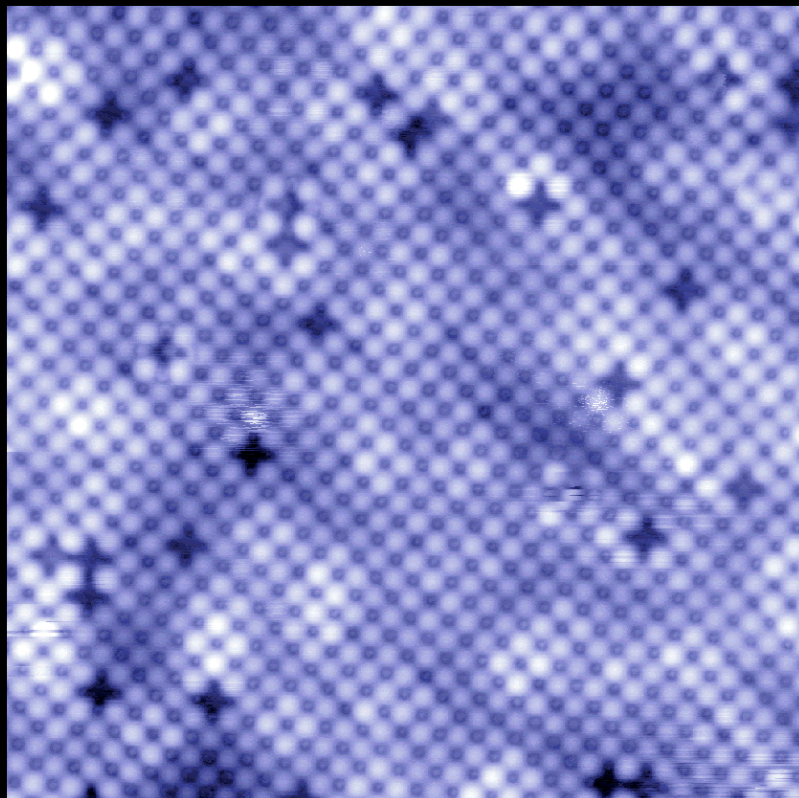
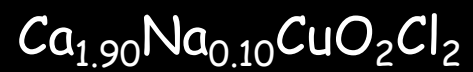
dI/dV Spectra



Intense Tunneling-Asymmetry (TA)
variation are highly similar

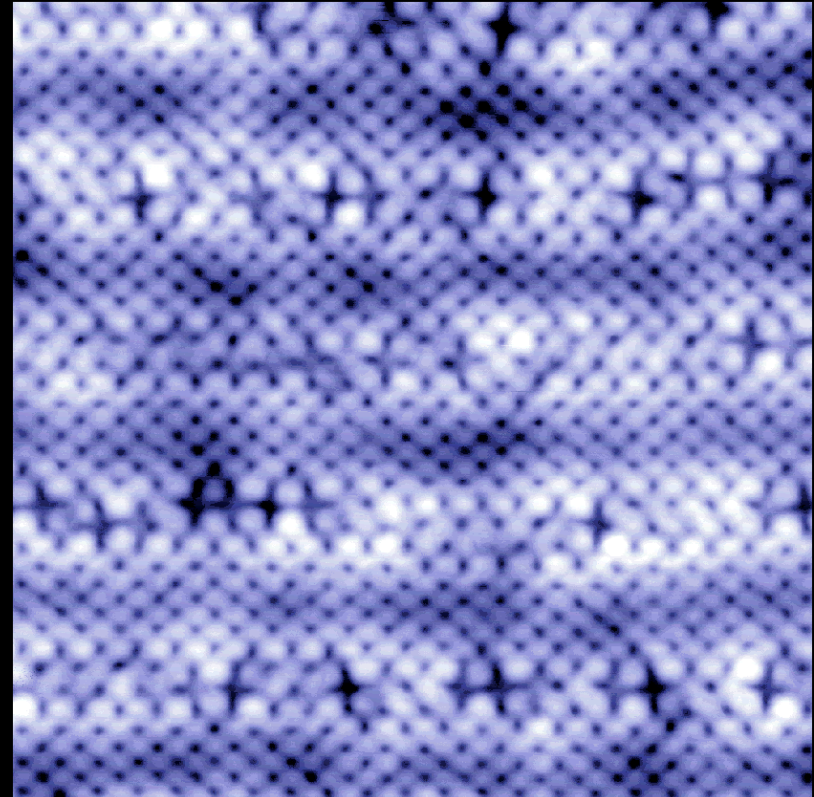
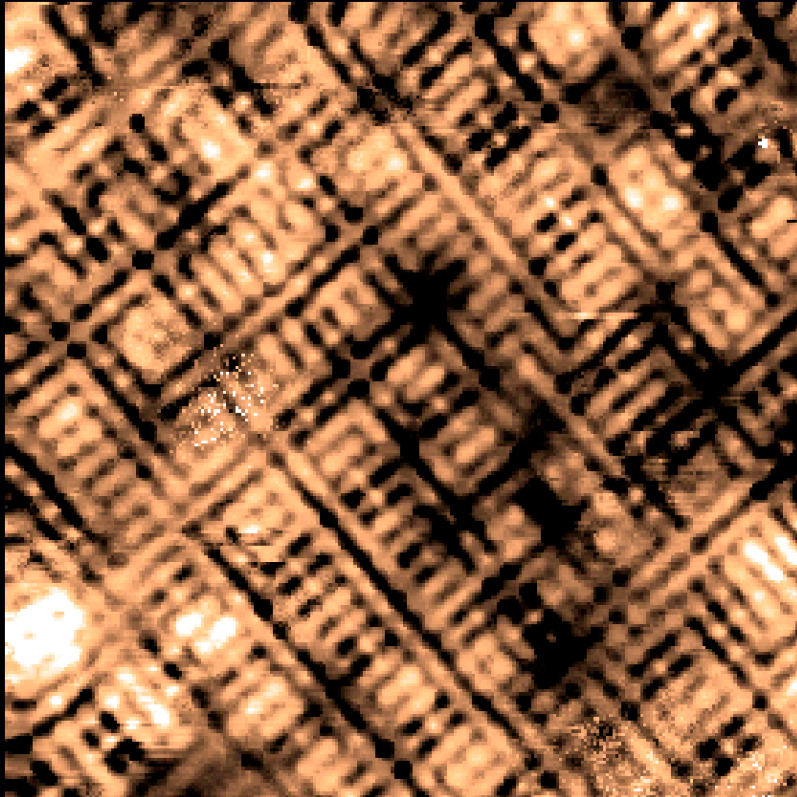
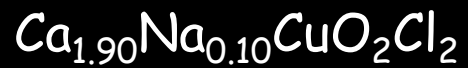
Y. Kohsaka et al. Science 315, 1380 (2007)

Topograph



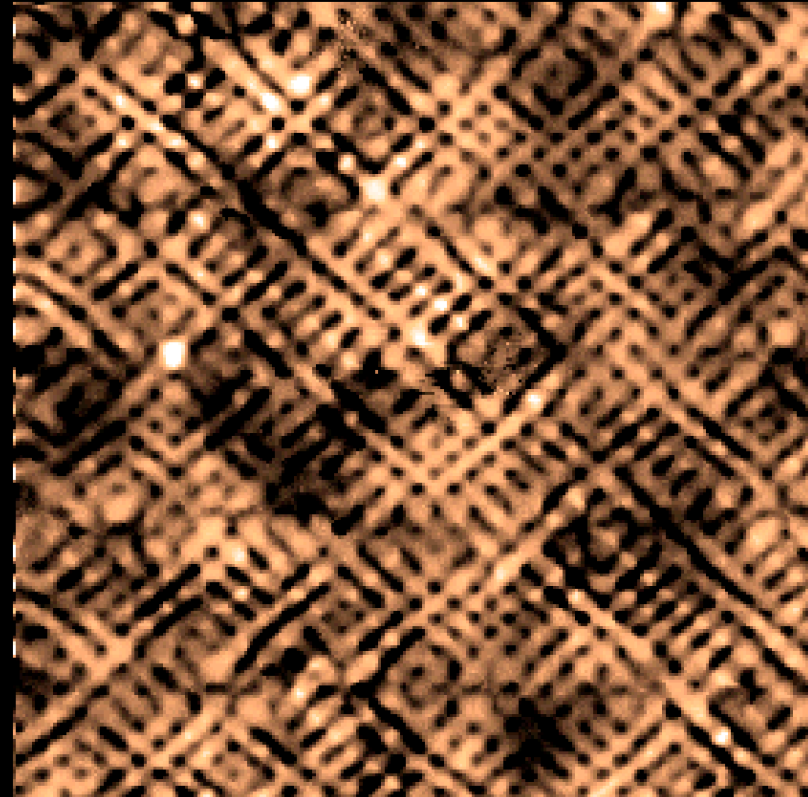
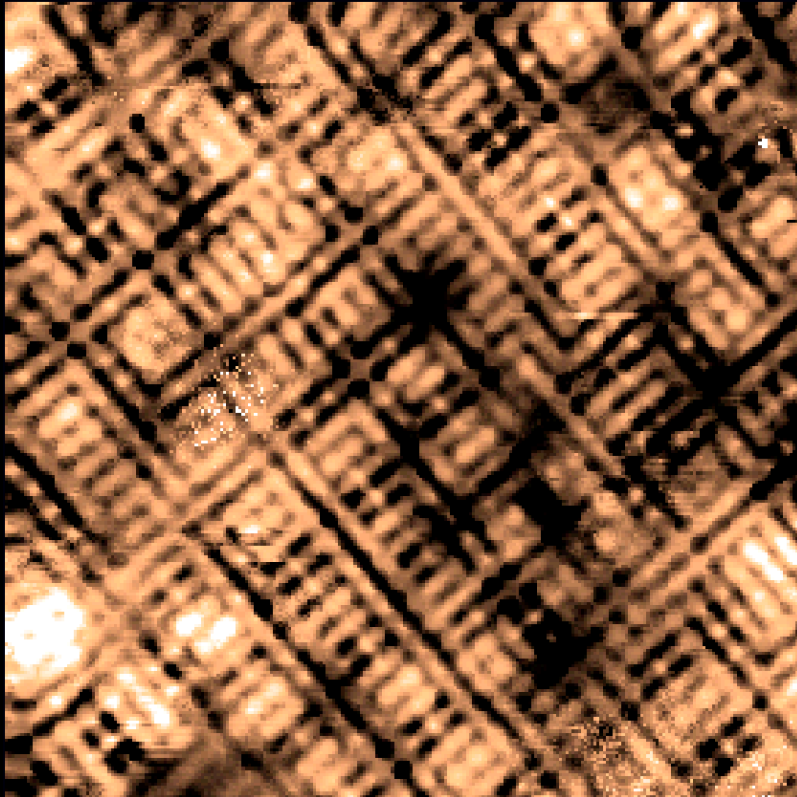
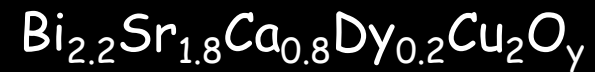
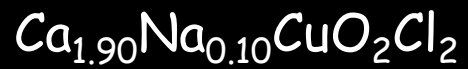
12 nm

Tunneling Asymmetry (TA)-map at $E=150\text{meV}$



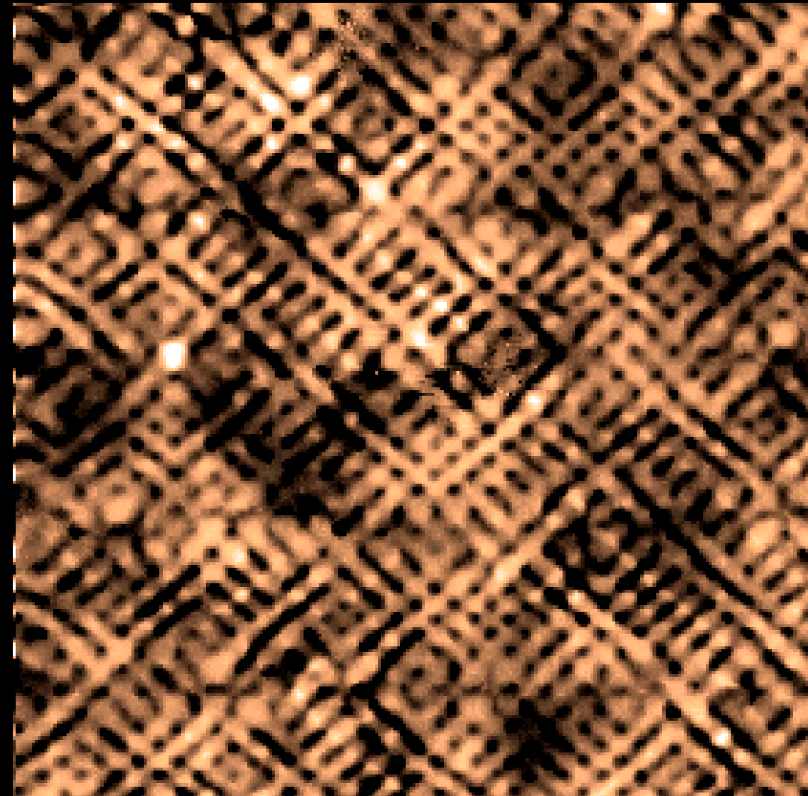
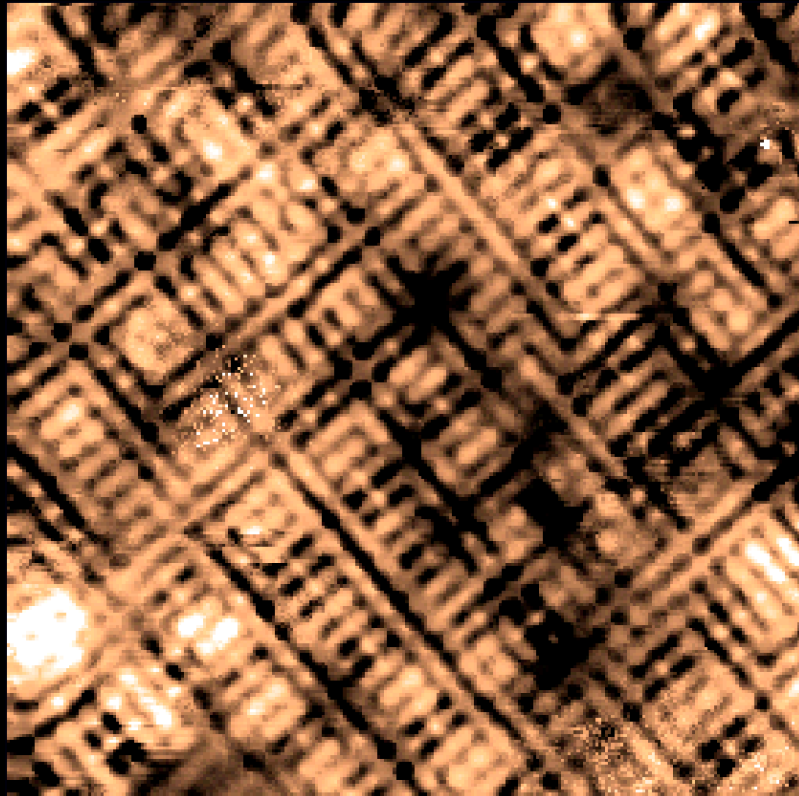
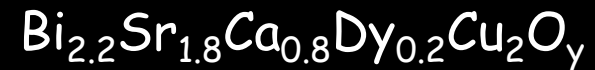
12 nm

Tunneling Asymmetry (TA)-map at $E=150\text{meV}$



12 nm

Tunneling Asymmetry (TA)-map at $E=150\text{meV}$



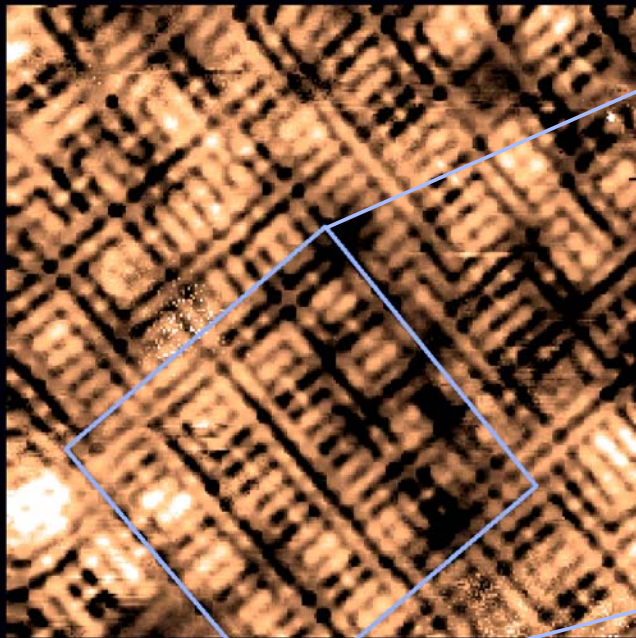
12 nm

Indistinguishable bond-centered TA contrast
with disperse $4a_0$ -wide nanodomains

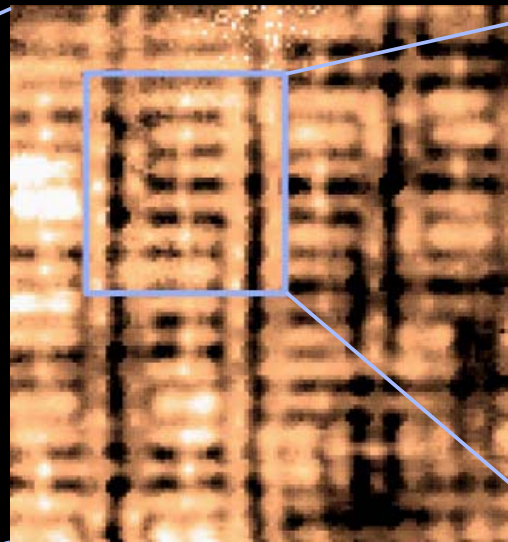
Y. Kohsaka et al. *Science* 315, 1380 (2007)

TA Contrast is at oxygen site (Cu-O-Cu bond-centered)

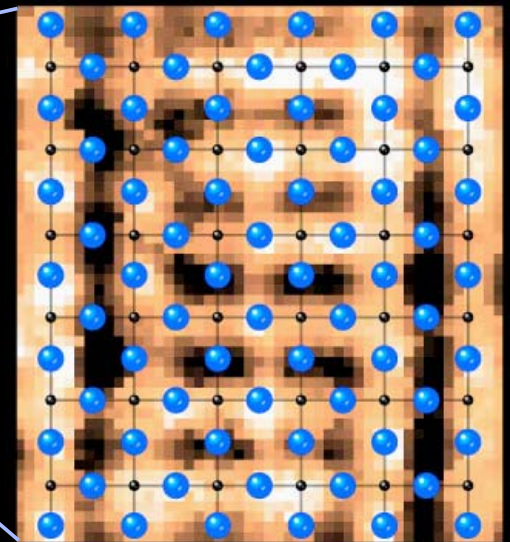
R map (150 mV)



12 nm



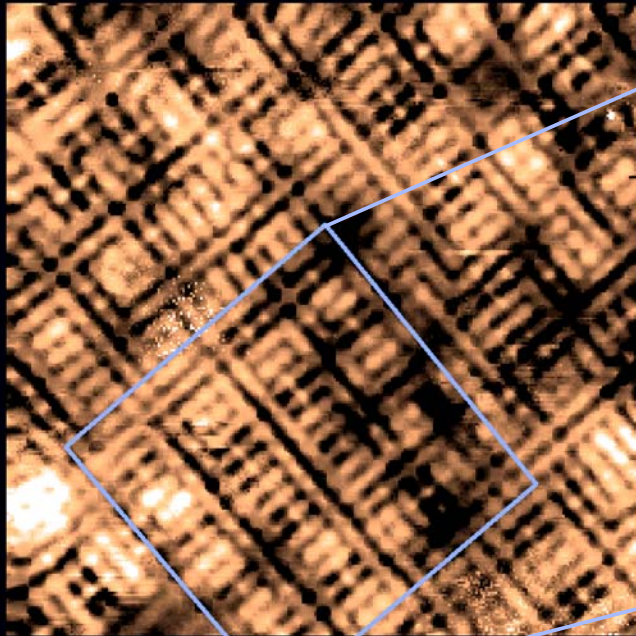
$\text{Ca}_{1.88}\text{Na}_{0.12}\text{CuO}_2\text{Cl}_2$, 4 K



$4a_0$

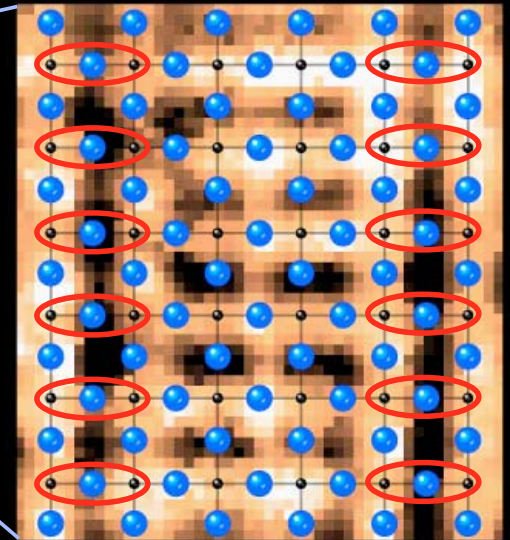
TA Contrast is at oxygen site (Cu-O-Cu bond-centered)

R map (150 mV)



← 12 nm →

$\text{Ca}_{1.88}\text{Na}_{0.12}\text{CuO}_2\text{Cl}_2$, 4 K

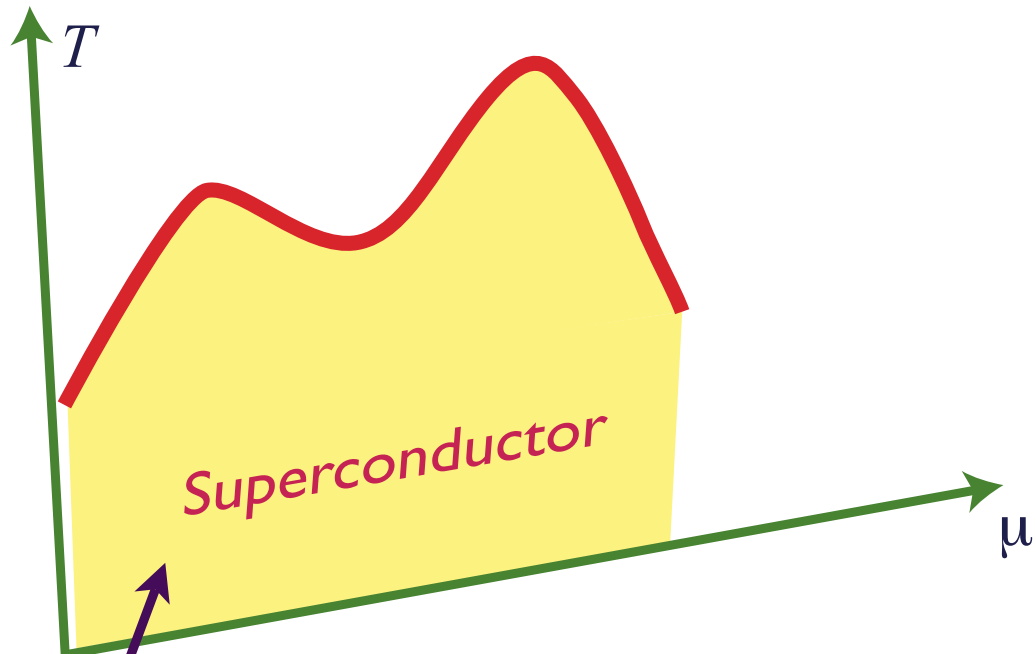


← $4a_0$ →

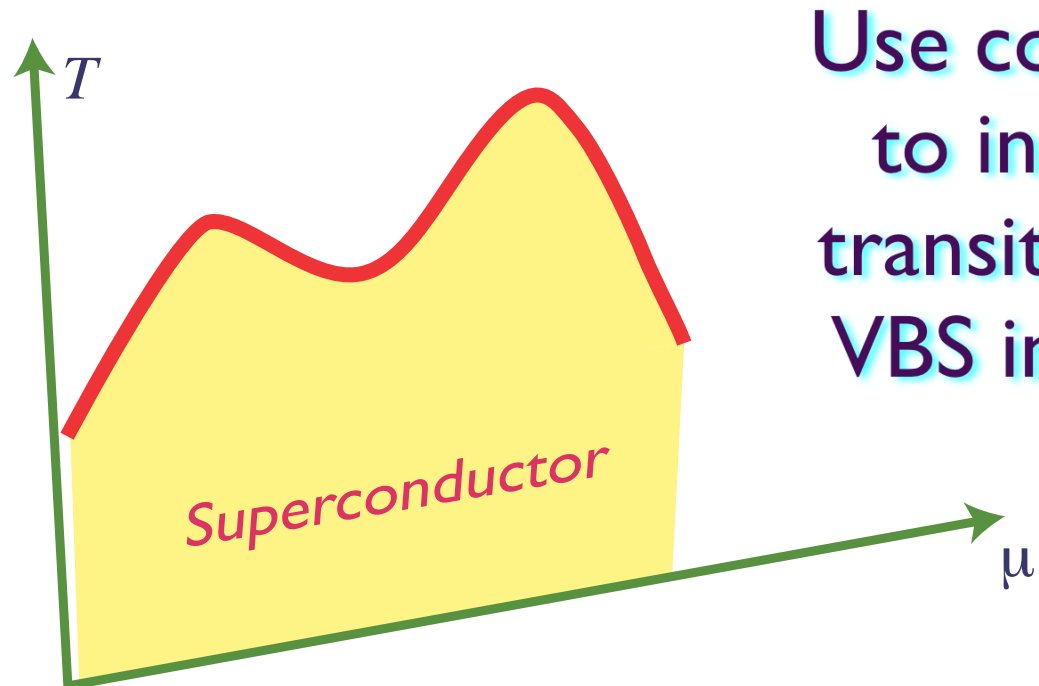
Evidence for a predicted valence bond supersolid

S. Sachdev and N. Read, *Int. J. Mod. Phys. B* **5**, 219 (1991).

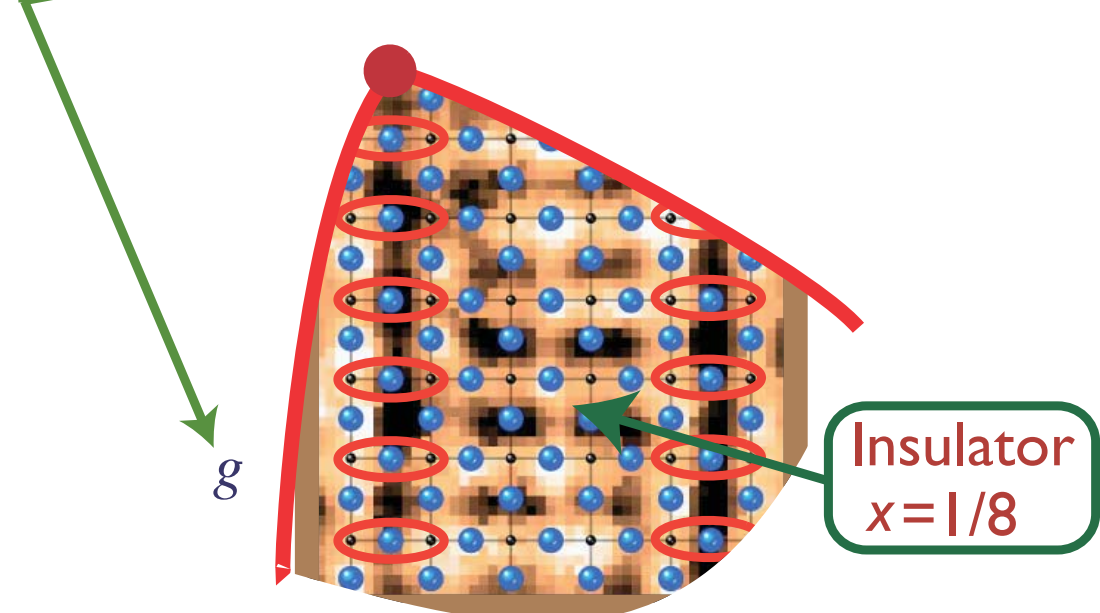
M. Vojta and S. Sachdev, *Phys. Rev. Lett.* **83**, 3916 (1999).

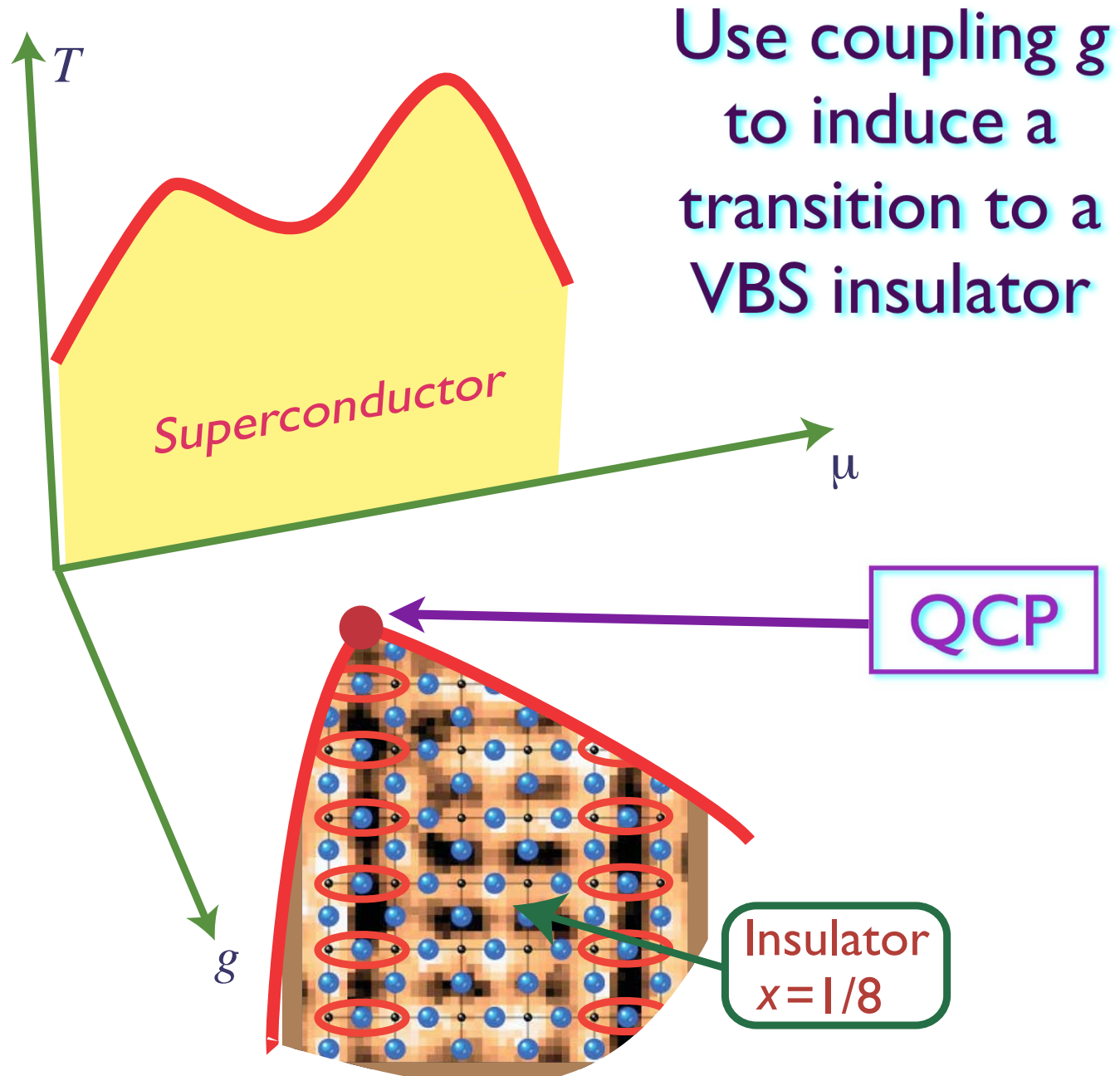


Scanning tunnelling microscopy

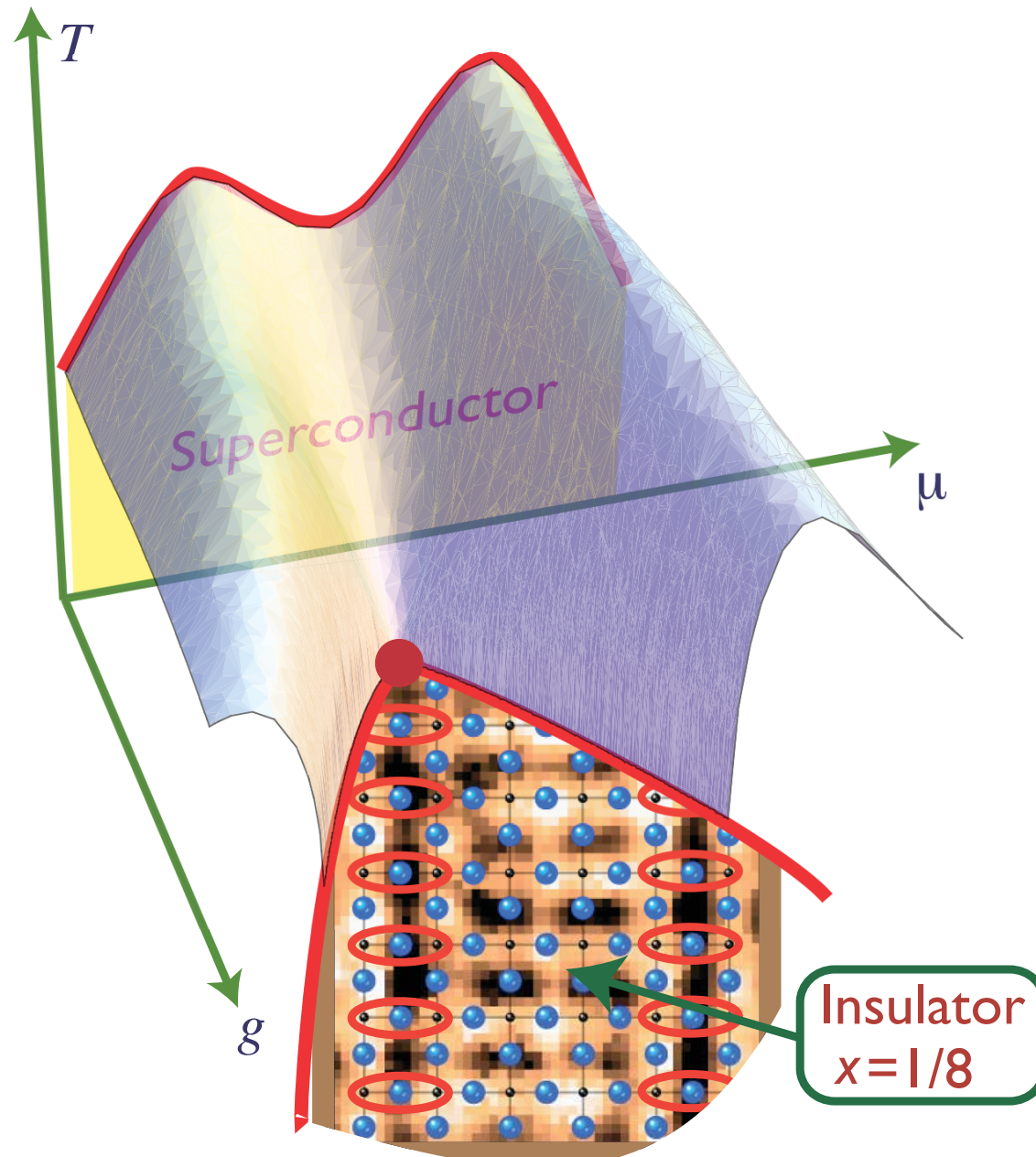


Use coupling g to induce a transition to a VBS insulator

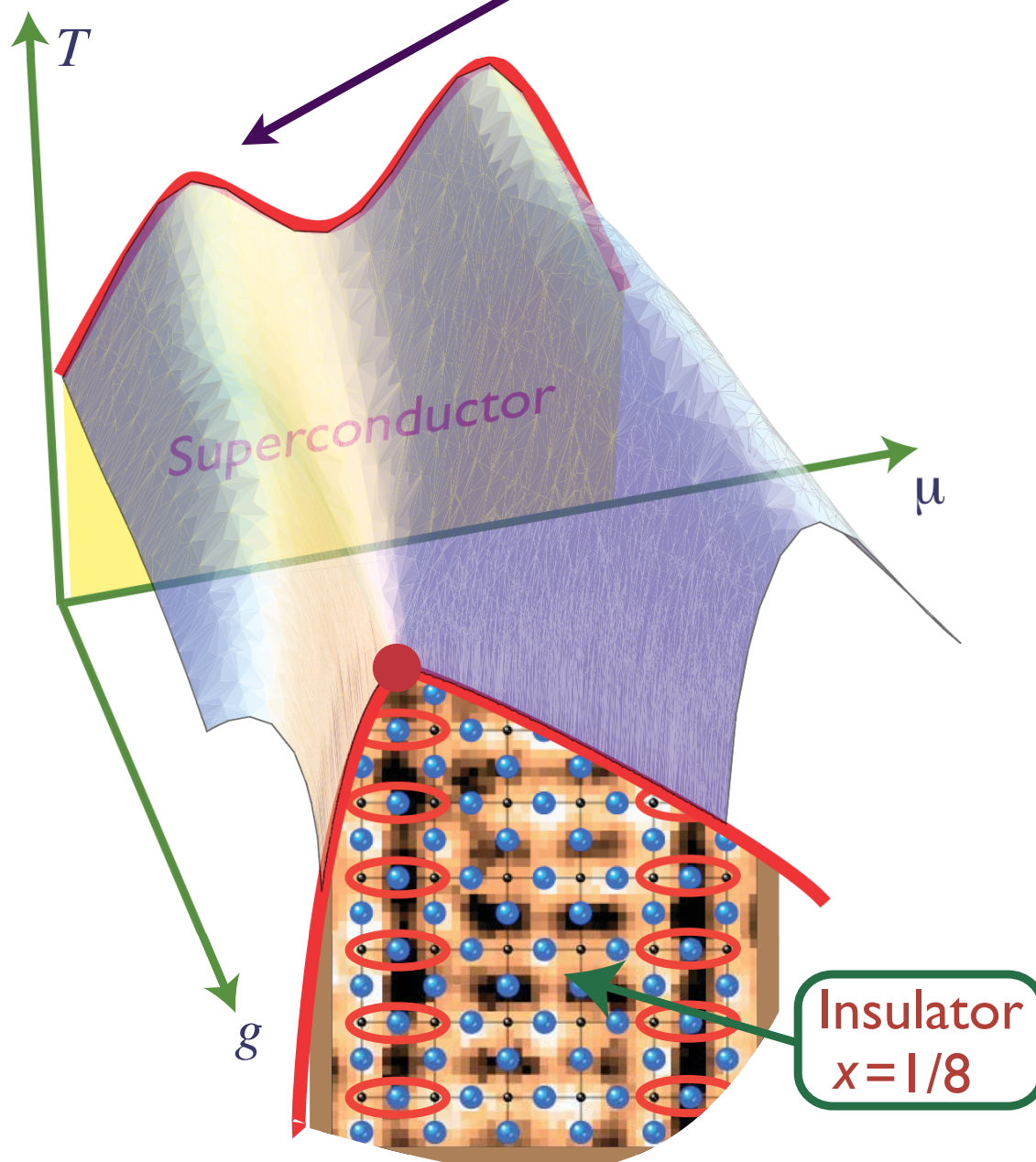




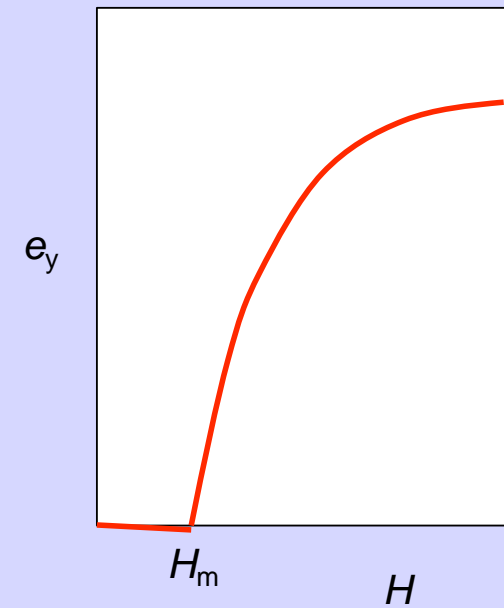
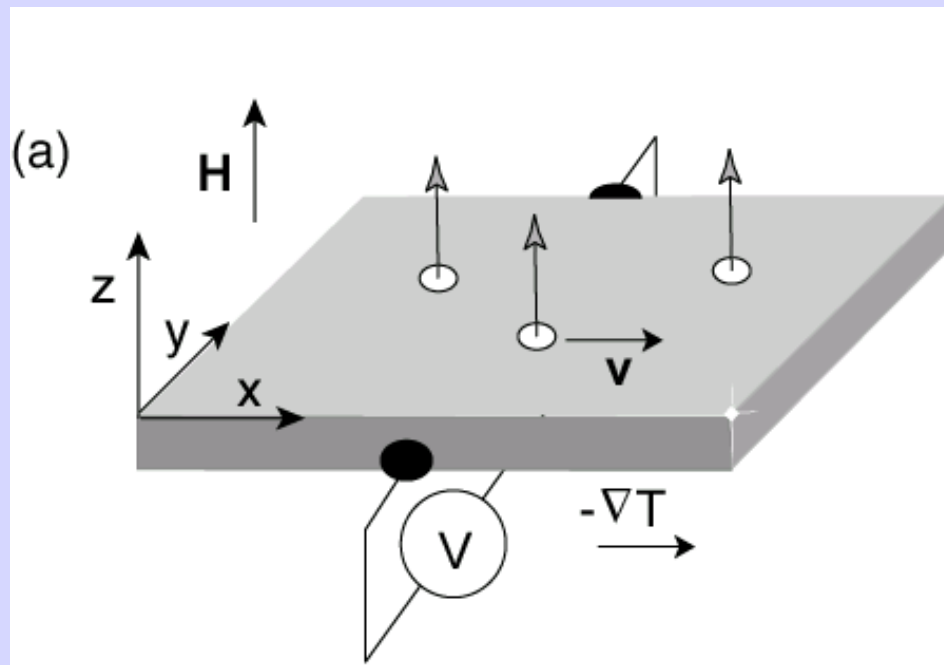
Proposed generalized phase diagram



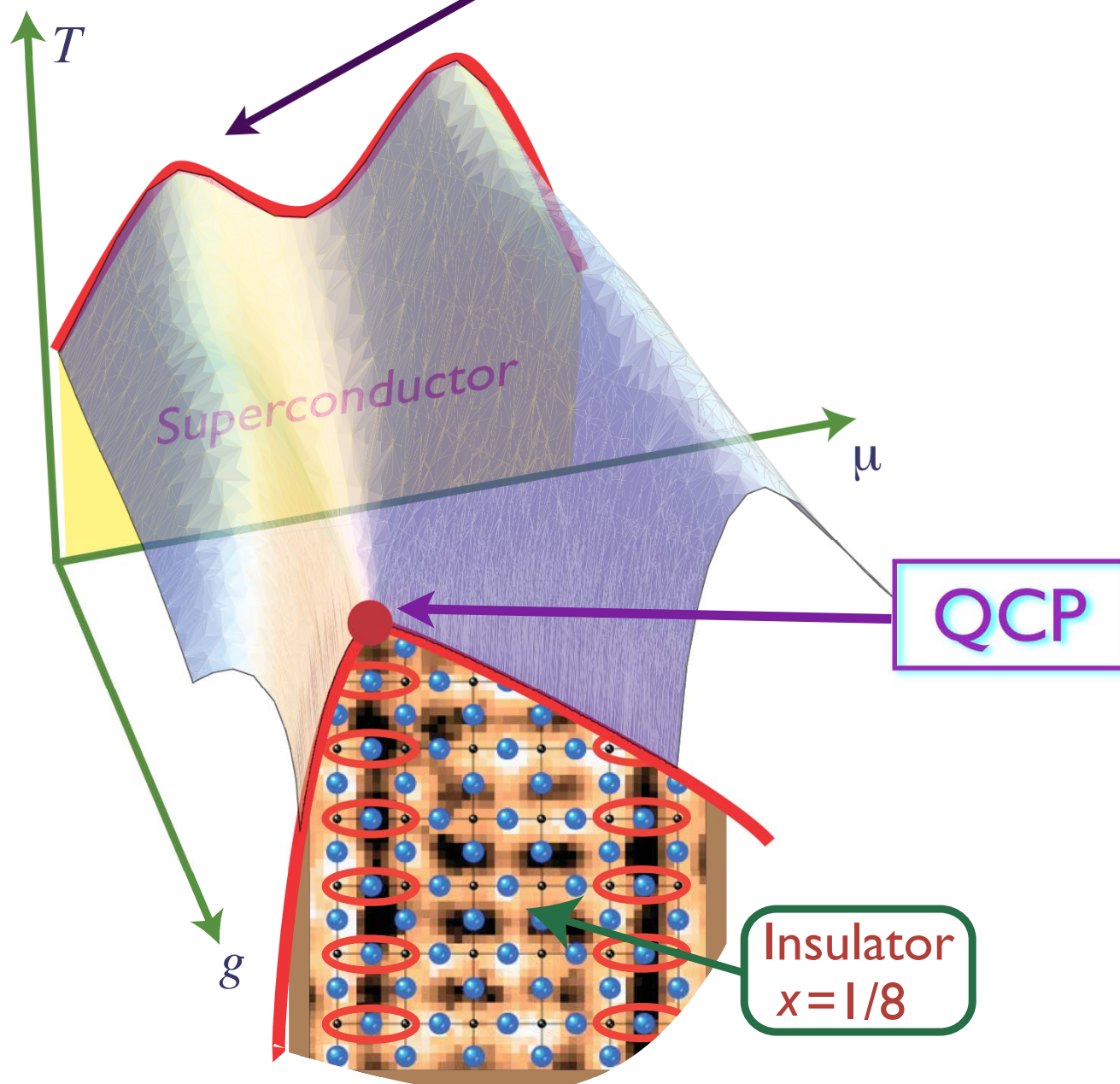
Nernst measurements



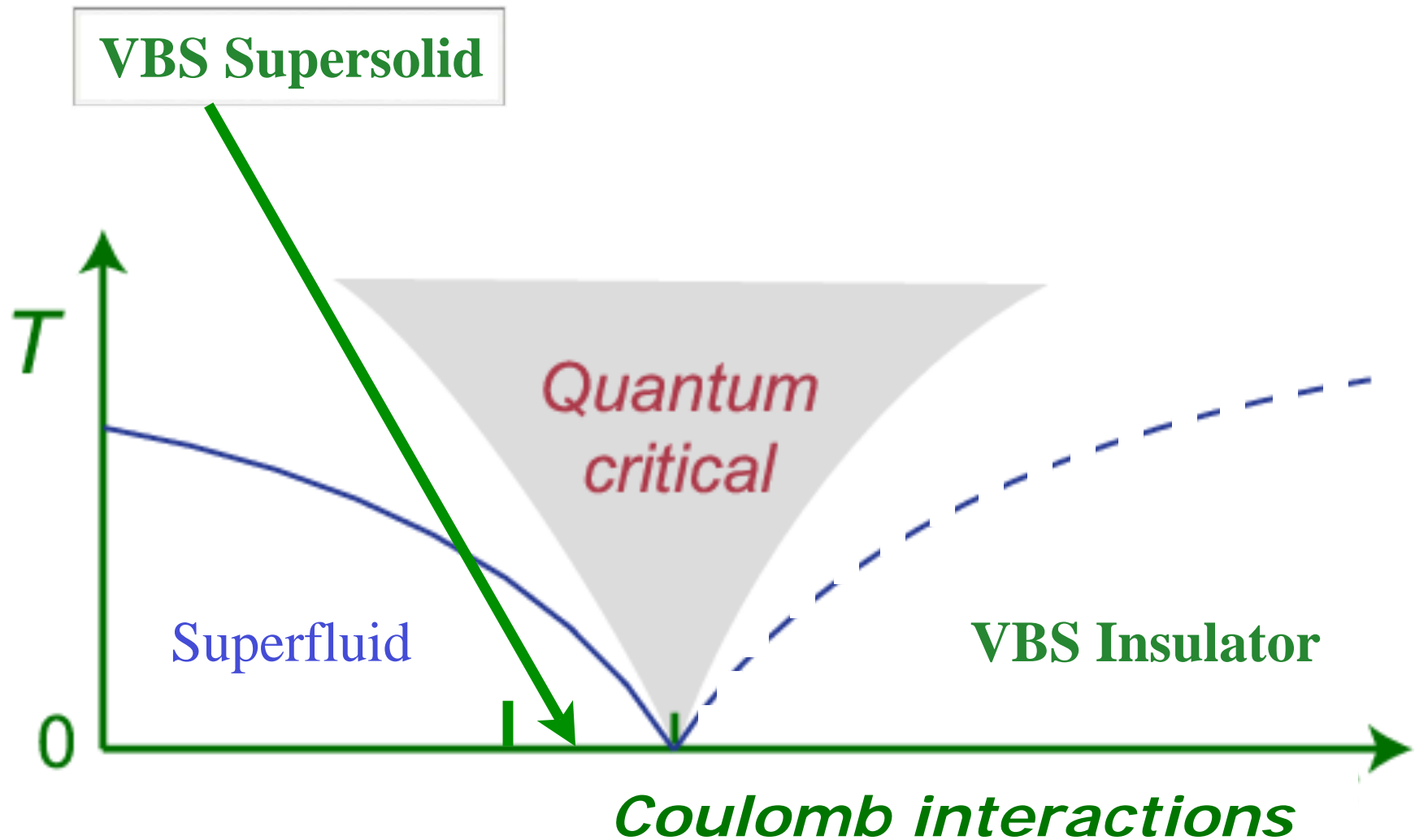
Nernst experiment



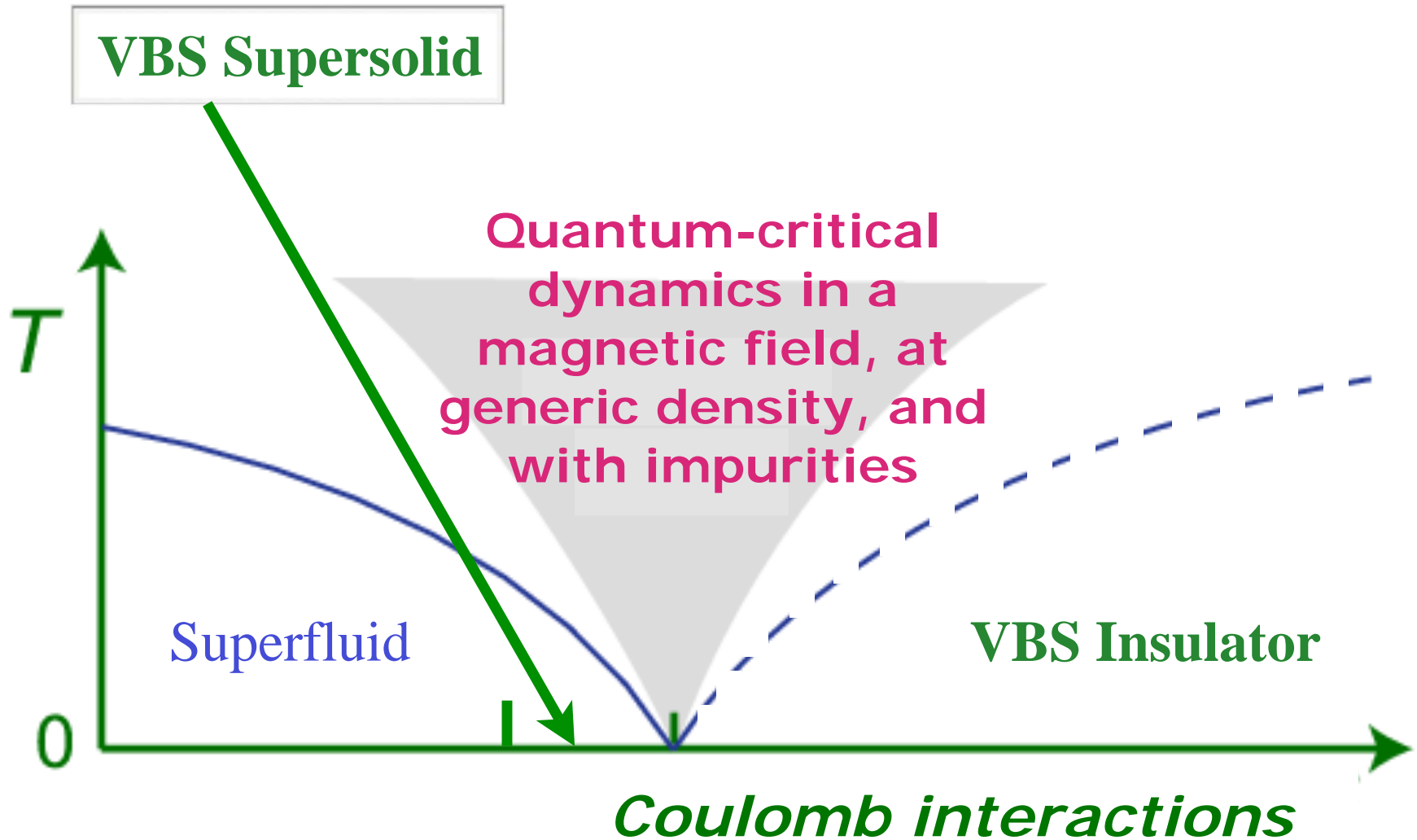
Nernst measurements



Non-zero temperature phase diagram



Non-zero temperature phase diagram



To the CFT of the quantum critical point, we add

- A chemical potential μ
- A magnetic field B

After the AdS/CFT mapping, we obtain the Einstein-Maxwell theory of a black hole with

- An electric charge
- A magnetic charge

A precise correspondence is found between general hydrodynamics of vortices near quantum critical points and solvable models of black holes with electric and magnetic charges

In the hydrodynamic regime, $\hbar\omega \ll k_B T$, we can use classical principles involving relaxation to local equilibrium to understand these perturbations.

The variables entering the hydrodynamic theory are

- the external magnetic field $F^{\mu\nu}$,

$$F^{\mu\nu} = \begin{pmatrix} 0 & 0 & 0 \\ 0 & 0 & B \\ 0 & -B & 0 \end{pmatrix},$$

- $T^{\mu\nu}$, the stress energy tensor,
- J^μ , the current,
- ρ , the local number density,
- ε , the local energy density,
- P , the local pressure,
- u^μ , the local velocity, and
- σ_Q , a universal conductivity, which is the **single transport co-efficient**.

The dependence of ε , P , σ_Q on T and v follows from simple scaling arguments

Lorentz invariance and positivity of entropy production lead to the hydrodynamic equations of motion and constitutive relations:

S.A. Hartnoll, P.K. Kovtun, M. Müller, and S. Sachdev, *Phys. Rev. B* **76** 144502 (2007)

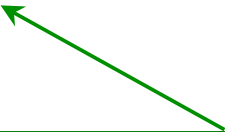
Lorentz invariance and positivity of entropy production lead to the hydrodynamic equations of motion and constitutive relations:

$$\begin{aligned}\partial_\mu J^\mu &= 0 \\ \partial_\mu T^{\mu\nu} &= F^{\mu\nu} J_\nu\end{aligned}$$

← Conservation laws/equations of motion

Lorentz invariance and positivity of entropy production lead to the hydrodynamic equations of motion and constitutive relations:

$$\begin{aligned}\partial_\mu J^\mu &= 0 \\ \partial_\mu T^{\mu\nu} &= F^{\mu\nu} J_\nu \\ T^{\mu\nu} &= (\varepsilon + P)u^\mu u^\nu + P g^{\mu\nu} \\ J^\mu &= \rho u^\mu\end{aligned}$$



Constitutive relations which follow from Lorentz transformation to moving frame

Lorentz invariance and positivity of entropy production lead to the hydrodynamic equations of motion and constitutive relations:

$$\begin{aligned}\partial_\mu J^\mu &= 0 \\ \partial_\mu T^{\mu\nu} &= F^{\mu\nu} J_\nu \\ T^{\mu\nu} &= (\varepsilon + P)u^\mu u^\nu + P g^{\mu\nu} \\ J^\mu &= \rho u^\mu + \sigma_Q (g^{\mu\nu} + u^\mu u^\nu) \left[(-\partial_\nu \mu + F_{\nu\lambda} u^\lambda) + \mu \frac{\partial_\mu T}{T} \right]\end{aligned}$$

Single dissipative term allowed by requirement of positive entropy production. There is only one independent transport co-efficient

Lorentz invariance and positivity of entropy production lead to the hydrodynamic equations of motion and constitutive relations:

$$\begin{aligned}
 \partial_\mu J^\mu &= 0 \\
 \partial_\mu T^{\mu\nu} &= F^{\mu\nu} J_\nu + \frac{1}{\tau_{\text{imp}}} (\delta_\nu^\mu + u^\mu u_\nu) T^{\nu\gamma} u_\gamma \\
 T^{\mu\nu} &= (\varepsilon + P) u^\mu u^\nu + P g^{\mu\nu} \\
 J^\mu &= \rho u^\mu + \sigma_Q (g^{\mu\nu} + u^\mu u^\nu) \left[(-\partial_\nu \mu + F_{\nu\lambda} u^\lambda) + \mu \frac{\partial_\mu T}{T} \right]
 \end{aligned}$$

Momentum relaxation from impurities

From these relations, we obtained results for the transport co-efficients, expressed in terms of a “cyclotron” frequency and damping:

$$\omega_c = \frac{2eB\rho v^2}{c(\varepsilon + P)} \quad , \quad \gamma = \frac{B^2 v^2}{c^2(\varepsilon + P)}$$

Transverse thermoelectric co-efficient

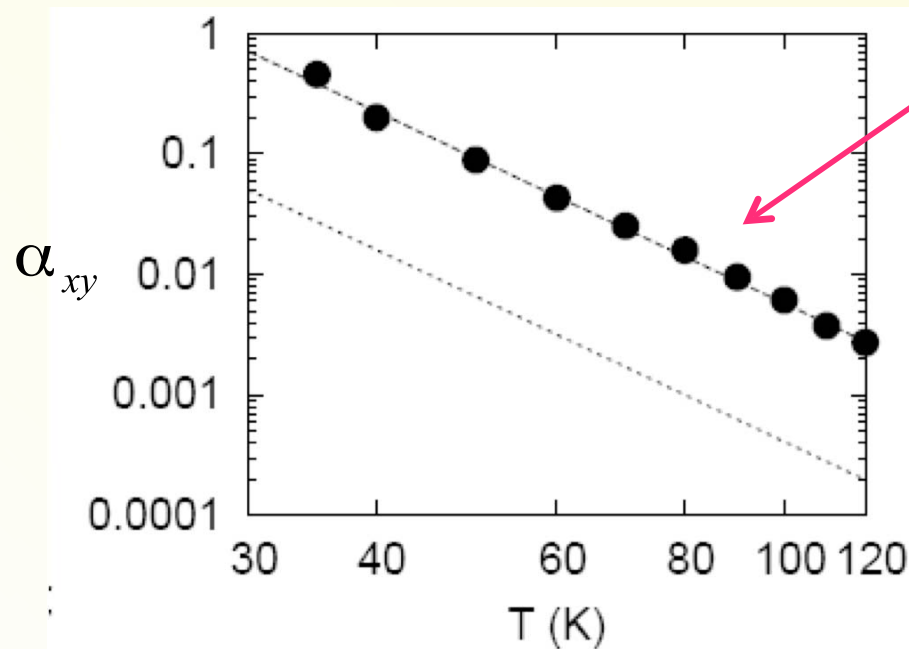
$$\left(\frac{h}{2ek_B}\right) \alpha_{xy} = \Phi_s \bar{B} (k_B T)^2 \left(\frac{2\pi\tau_{\text{imp}}}{\hbar}\right)^2 \frac{\bar{\rho}^2 + \Phi_\sigma \Phi_{\varepsilon+P} (k_B T)^3 \hbar / 2\pi\tau_{\text{imp}}}{\Phi_{\varepsilon+P}^2 (k_B T)^6 + \bar{B}^2 \bar{\rho}^2 (2\pi\tau_{\text{imp}}/\hbar)^2},$$

where

$$B = \bar{B}\phi_0/(\hbar v)^2 \quad ; \quad \rho = \bar{\rho}/(\hbar v)^2.$$

LSCO Experiments

Measurement of $\alpha_{xy} \approx \sigma_{xx} e_N$



Y. Wang et al., Phys. Rev. B 73, 024510 (2006).

$$\alpha_{xy} \propto \frac{1}{T^4}$$

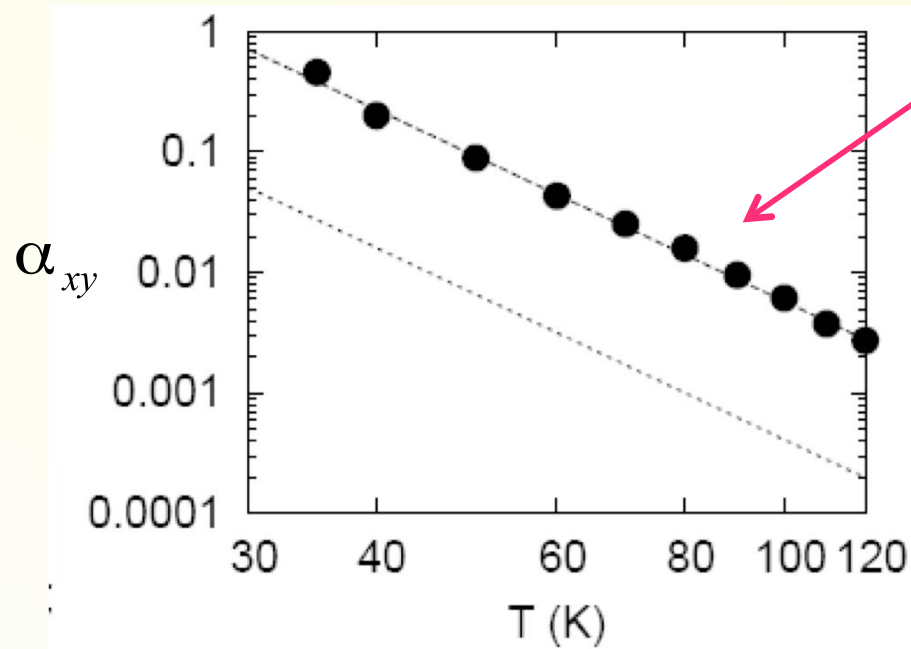
$$\alpha_{xy} \propto \frac{BT^2 (\# \rho^2 \tau_{imp} + \# T^3)}{T^6 + \# B^2 \rho^2 \tau_{imp}^2}$$

(T small)

$$\frac{\alpha_{xy}(B \rightarrow 0)}{B} \approx \left(\frac{2ek_B}{h\phi_0} \right) \frac{\Phi_s}{\Phi_{\varepsilon+P}^2} \left(\frac{2\pi\tau_{imp}}{\hbar} \right)^2 \frac{\rho^2 (\hbar v)^6}{(k_B T)^4}$$

LSCO Experiments

Measurement of $\alpha_{xy} \approx \sigma_{xx} e_N$



Y. Wang et al., Phys. Rev. B 73, 024510 (2006).

$$\alpha_{xy} \propto \frac{1}{T^4}$$

$$\alpha_{xy} \propto \frac{BT^2 (\#\rho^2\tau_{imp} + \#T^3)}{T^6 + \#B^2\rho^2\tau_{imp}^2}$$

(T small)

$$\frac{\alpha_{xy}(B \rightarrow 0)}{B} \approx \left(\frac{2ek_B}{h\phi_0} \right) \frac{\Phi_s}{\Phi_{\varepsilon+P}^2} \left(\frac{2\pi\tau_{imp}}{\hbar} \right)^2 \frac{\rho^2(\hbar v)^6}{(k_B T)^4}$$

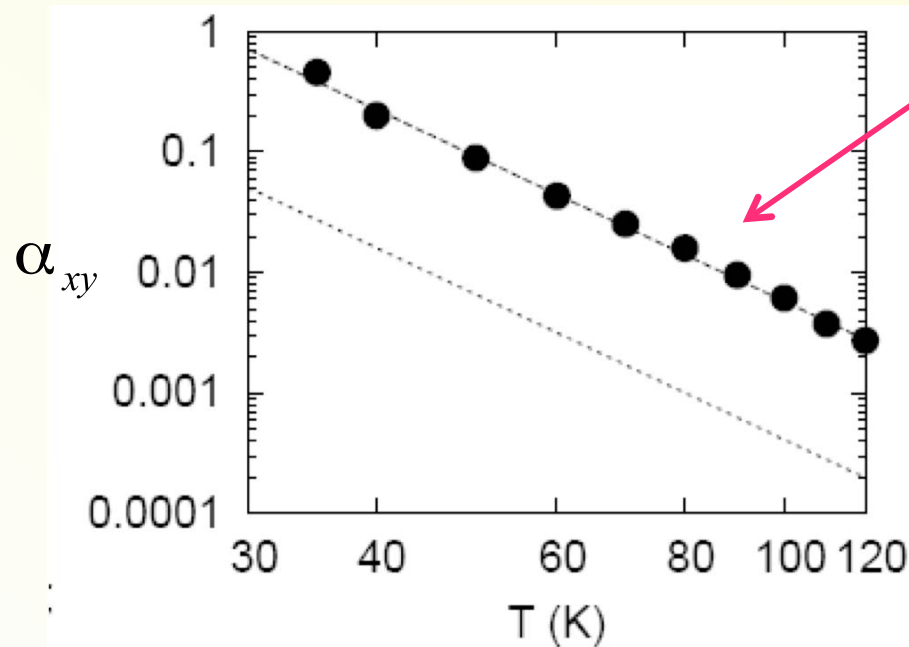
$$\hbar v \approx 47 \text{ meV } \overset{\circ}{\text{A}}$$

$$v \approx 2.5 \times 10^{-5} c$$

$$\tau_{imp} \approx 10^{-12} \text{ s}$$

LSCO Experiments

Measurement of $\alpha_{xy} \approx \sigma_{xx} e_N$



Y. Wang et al., Phys. Rev. B 73, 024510 (2006).

→ Prediction for ω_c :

$$\omega_c = 6.2 \text{ GHz} \frac{B}{1 \text{ T}} \left(\frac{35 \text{ K}}{T} \right)^3$$

$$\alpha_{xy} \propto \frac{BT^2 (\# \rho^2 \tau_{imp} + \# T^3)}{T^6 + \# B^2 \rho^2 \tau_{imp}^2}$$

(T small)

$$\frac{\alpha_{xy}}{B} (B \rightarrow 0) \approx \left(\frac{2ek_B}{h\phi_0} \right) \frac{\Phi_s}{\Phi_{\varepsilon+P}^2} \left(\frac{2\pi\tau_{imp}}{\hbar} \right)^2 \rho^2 (\hbar v)^6 \underbrace{(k_B T)^4}$$

$$\hbar v \approx 47 \text{ meV } \overset{\circ}{\text{A}}$$

$$v \approx 2.5 \times 10^{-5} c$$

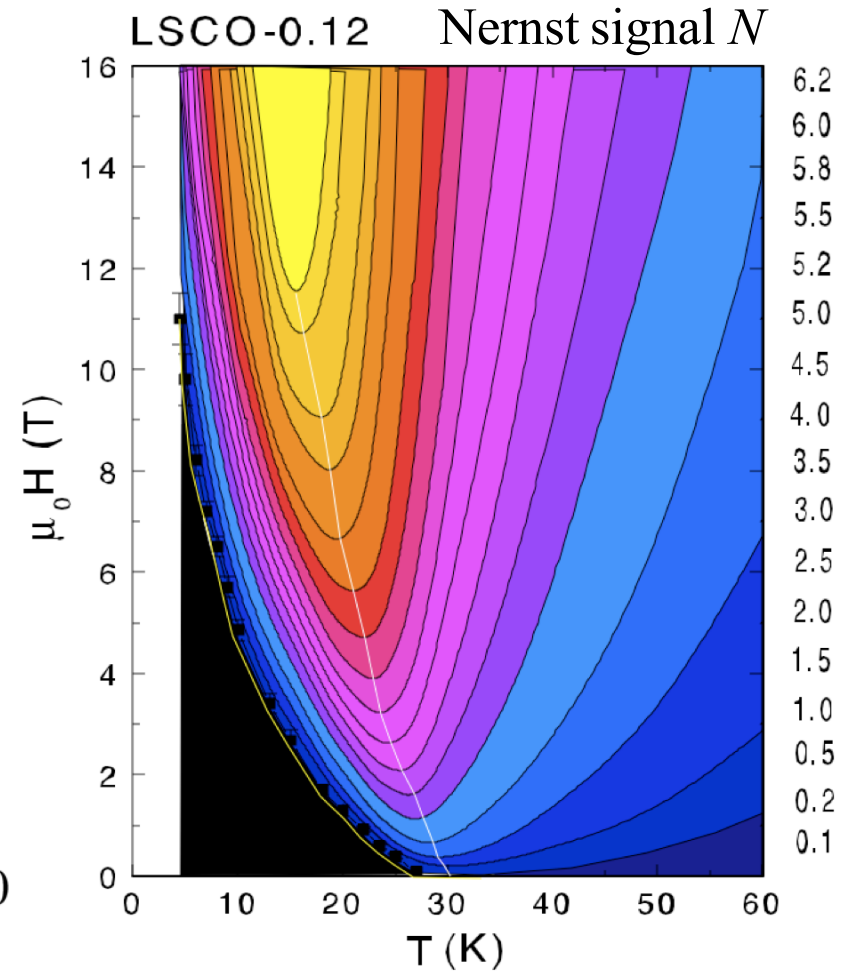
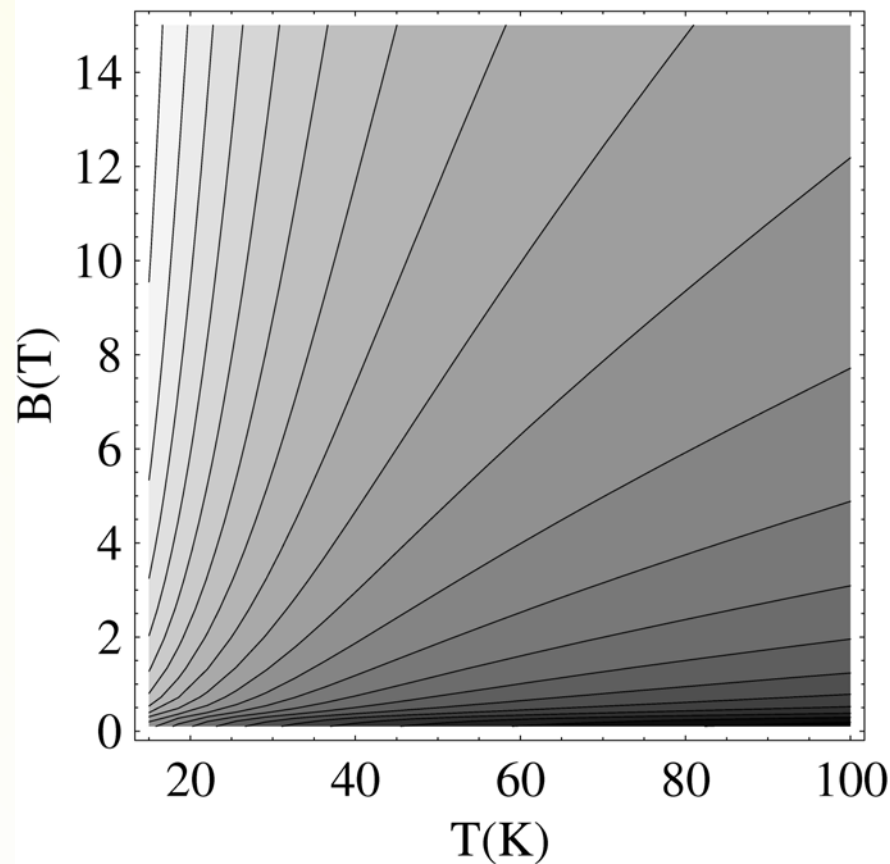
$$\tau_{imp} \approx 10^{-12} \text{ s}$$

- **T-dependent** cyclotron frequency!
- 0.035 times **smaller** than the cyclotron frequency of free electrons (at T=35 K)
- Only observable **in ultra-pure samples** where $\tau_{imp}^{-1} \leq \omega_c$

LSCO Experiments

B, T -dependence

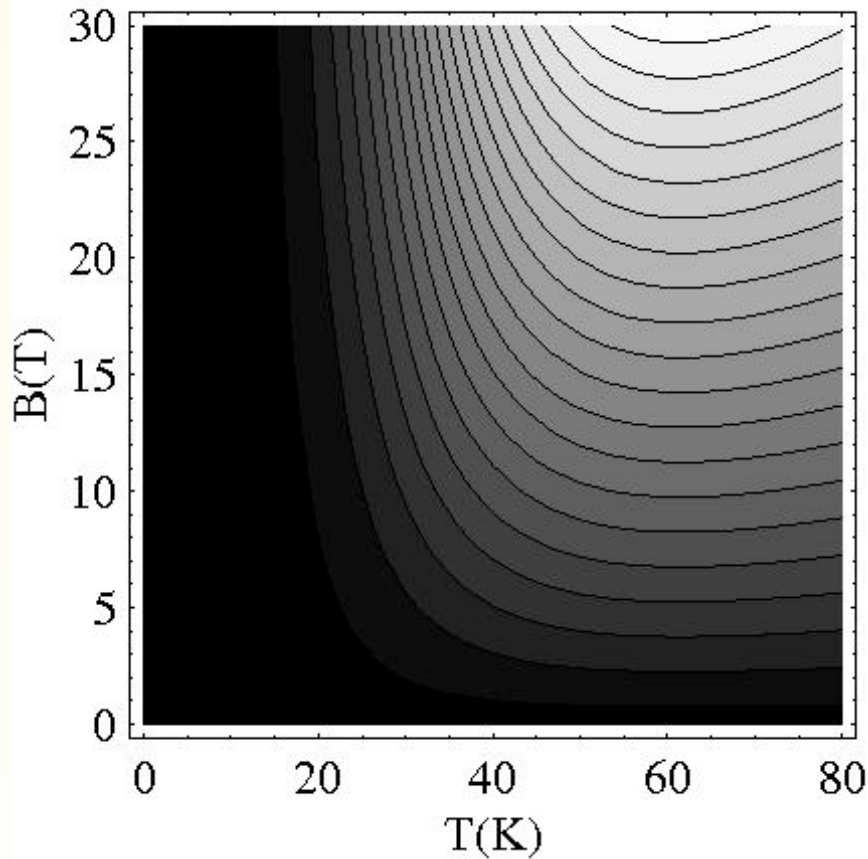
Theory for $\alpha_{xy} \approx \sigma_{xx} N$



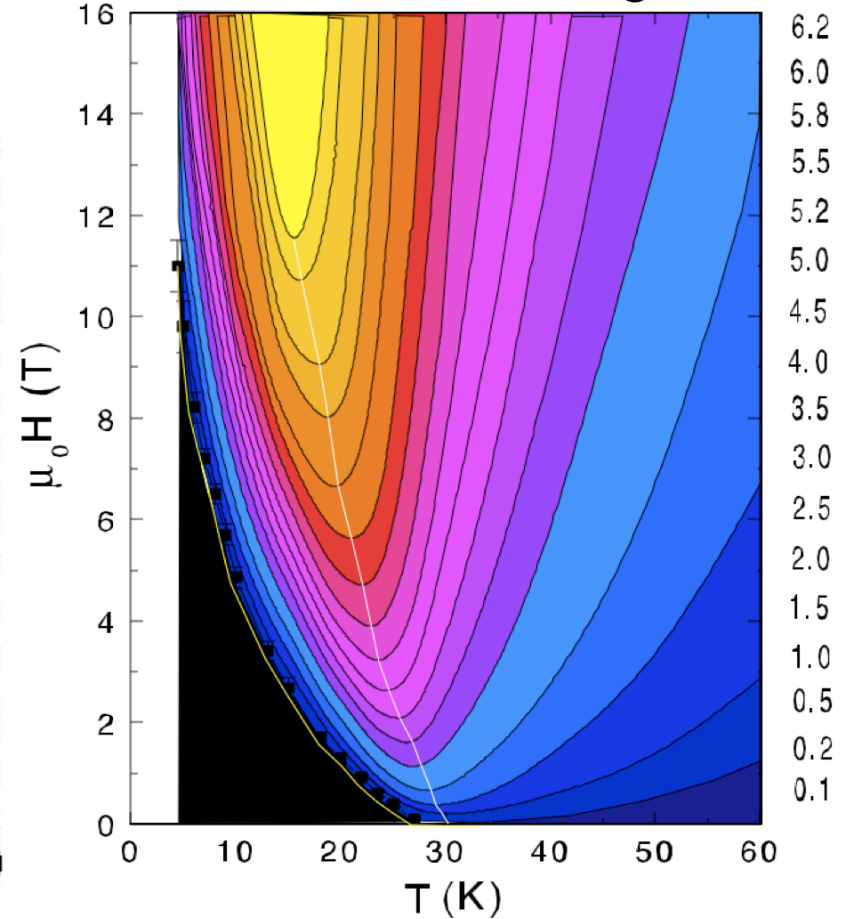
Y. Wang, L. Li, and N. P. Ong, Phys. Rev. B 73, 024510 (2006).

LSCO Experiments

Theory for N



LSCO-0.12 Nernst signal N



Y. Wang, L. Li, and N. P. Ong, Phys. Rev. B 73, 024510 (2006).

To the CFT of the quantum critical point, we add

- A chemical potential μ
- A magnetic field B

After the AdS/CFT mapping, we obtain the Einstein-Maxwell theory of a black hole with

- An electric charge
- A magnetic charge

A precise correspondence is found between general hydrodynamics of vortices near quantum critical points and solvable models of black holes with electric and magnetic charges

Outline

1. Entanglement of spins

Experiments on antiferromagnetic insulators

2. Black Hole Thermodynamics

Connections to quantum criticality

3. Nernst effect in the cuprate superconductors

Quantum criticality and dyonic black holes

4. Quantum criticality in graphene

Hydrodynamic cyclotron resonance and Nernst effect

Outline

1. Entanglement of spins

Experiments on antiferromagnetic insulators

2. Black Hole Thermodynamics

Connections to quantum criticality

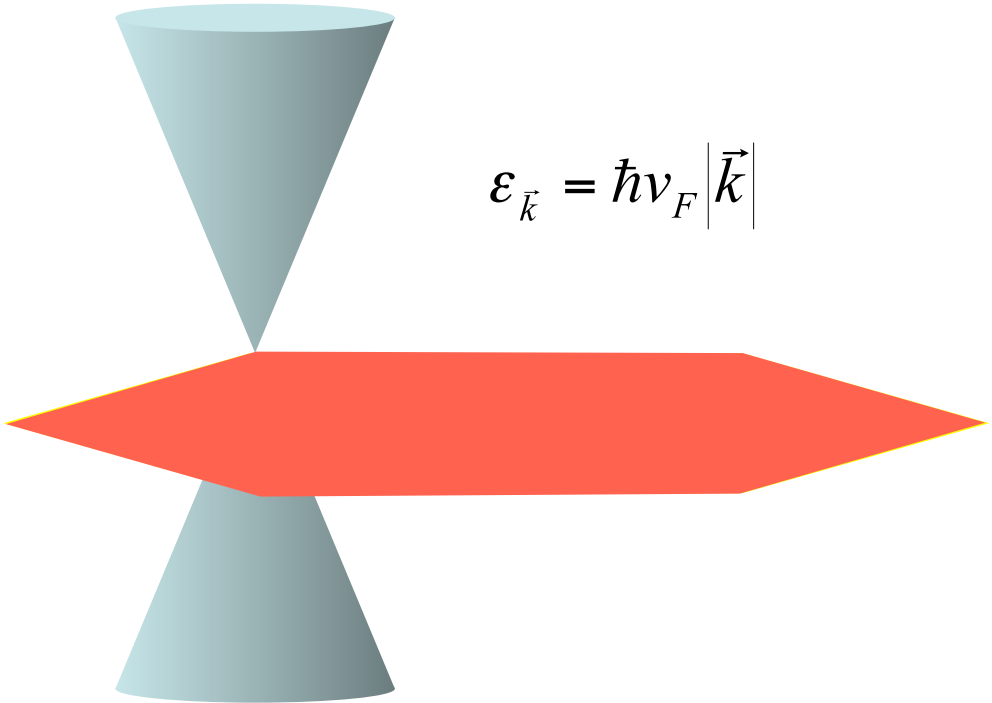
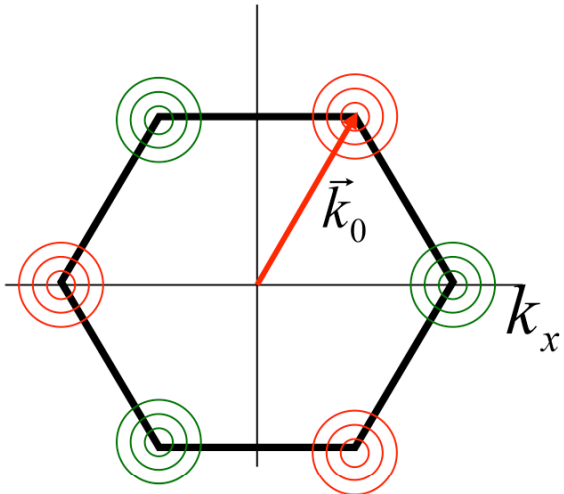
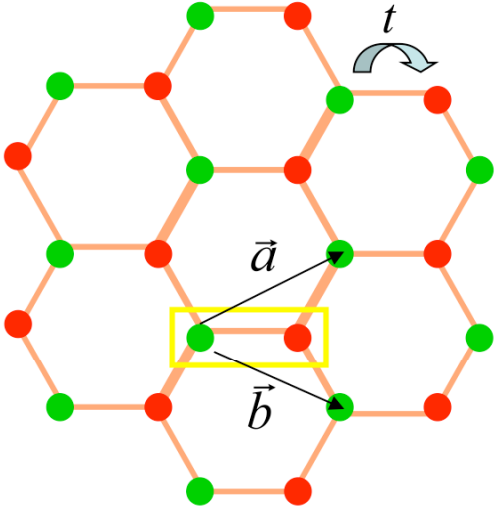
3. Nernst effect in the cuprate superconductors

Quantum criticality and dyonic black holes

4. Quantum criticality in graphene

Hydrodynamic cyclotron resonance and Nernst effect

Graphene



$$\varepsilon_{\vec{k}} = \hbar v_F |\vec{k}|$$

Graphene

Low energy theory has 4 two-component Dirac fermions, ψ_α , $\alpha = 1 \dots 4$, interacting with a $1/r$ Coulomb interaction

$$\mathcal{S} = \int d^2r d\tau \psi_\alpha^\dagger \left(\partial_\tau - i v_F \vec{\sigma} \cdot \vec{\nabla} \right) \psi_\alpha + \frac{e^2}{2} \int d^2r d^2r' d\tau \psi_\alpha^\dagger \psi_\alpha(r) \frac{1}{|r - r'|} \psi_\beta^\dagger \psi_\beta(r')$$

Dimensionless “fine-structure” constant $\lambda = e^2 / (4\hbar v_F)$.

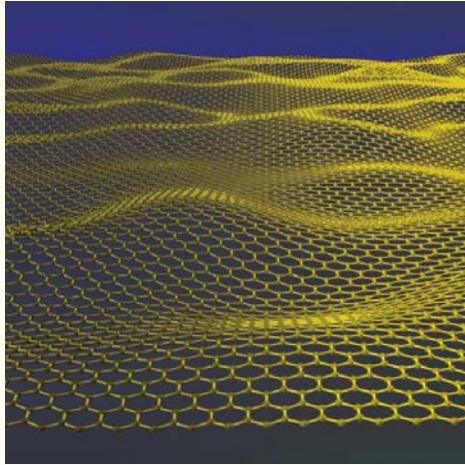
RG flow of λ :

$$\frac{d\lambda}{d\ell} = -\lambda^2 + \dots$$

Behavior is similar to a CFT3 with $\lambda \sim 1 / \ln(\text{scale})$

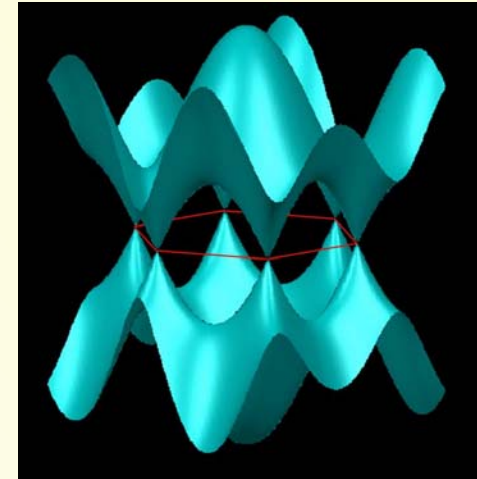
Cyclotron resonance in graphene

M. Mueller, and S. Sachdev, arXiv:0801.2970.



$$\omega = \pm\omega_c^{rel} - i\gamma - i/\tau$$

$$v = 1.1 \times 10^6 \text{ m/s} \\ \approx c/300$$



Conditions to observe resonance

- Negligible Landau quantization
- Hydrodynamic, collision-dominated regime
- Negligible broadening
- Relativistic, quantum critical regime

$$E_{LL} = \hbar v \sqrt{\frac{2eB}{\hbar c}} \ll k_B T$$

$$\hbar\omega_c^{rel} \ll k_B T$$

$$\gamma, \tau^{-1} < \omega_c^{rel}$$

$$\rho \leq \rho_{th} = \frac{(k_B T)^2}{(\hbar v)^2}$$

$$T \approx 300 \text{ K}$$

$$B \approx 0.1 \text{ T}$$

$$\rho \approx 10^{11} \text{ cm}^{-2}$$

$$\omega_c \approx 10^{13} \text{ s}^{-1}$$

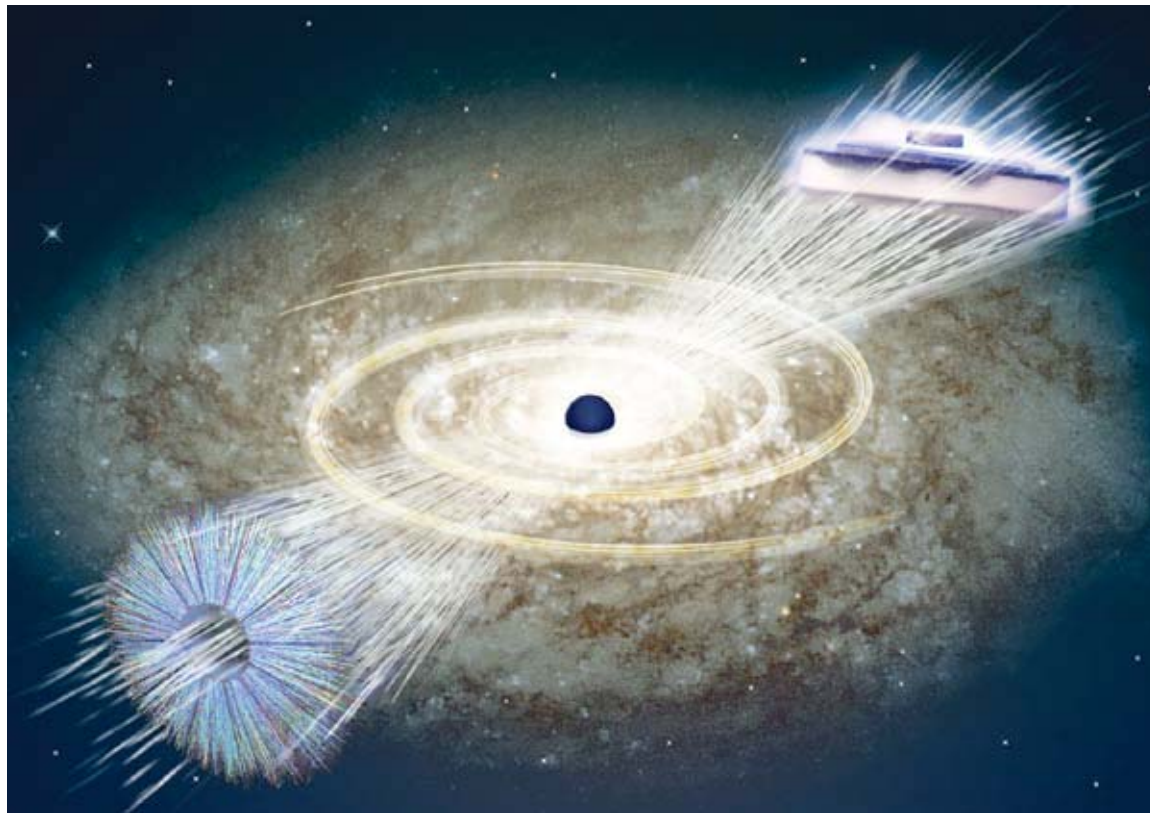
THEORETICAL PHYSICS

A black hole full of answers

Jan Zaanen

A facet of string theory, the currently favoured route to a 'theory of everything', might help to explain some properties of exotic matter phases — such as some peculiarities of high-temperature superconductors.

NATURE|Vol 448|30 August 2007



Conclusions

- Quantum phase transitions in antiferromagnets
- Exact solutions via black hole mapping have yielded first exact results for transport co-efficients in interacting many-body systems, and were valuable in determining general structure of hydrodynamics.
- Theory of VBS order and Nernst effect in cuprates.
- Quantum-critical transport in graphene.